

**A DEFINITIVE GENERIC STUDY OF AUGMENTED
HORIZONTAL AXIS WIND ENERGY SYSTEMS**

Executive Summary. Final Report

By
Peter B. S. Lissaman
Bart Hibbs
Stel N. Walker
Thomas Zambrano

**NATIONAL RENEWABLE ENERGY LABORATORY
LIBRARY**

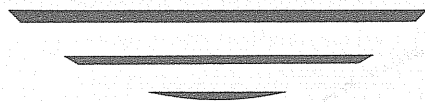
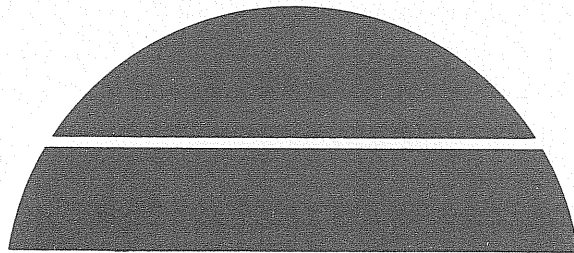
APR 08 1998

GOLDEN, COLORADO 80401-3393

April 1979

Work Performed Under Contract No. EG-77-C-01-4042

AeroVironment Inc.
Pasadena, California



U.S. Department of Energy



Solar Energy

DISCLAIMER

"This book was prepared as an account of work sponsored by an agency of the United States Government. Neither the United States Government nor any agency thereof, nor any of their employees, makes any warranty, express or implied, or assumes any legal liability or responsibility for the accuracy, completeness, or usefulness of any information, apparatus, product, or process disclosed, or represents that its use would not infringe privately owned rights. Reference herein to any specific commercial product, process, or service by trade name, trademark, manufacturer, or otherwise, does not necessarily constitute or imply its endorsement, recommendation, or favoring by the United States Government or any agency thereof. The views and opinions of authors expressed herein do not necessarily state or reflect those of the United States Government or any agency thereof."

This report has been reproduced directly from the best available copy.

Available from the National Technical Information Service, U. S. Department of Commerce, Springfield, Virginia 22161.

Price: Paper Copy \$7.00
Microfiche \$3.50

A DEFINITIVE GENERIC STUDY OF AUGMENTED
HORIZONTAL AXIS WIND ENERGY SYSTEMS

EXECUTIVE SUMMARY. FINAL REPORT

APRIL 1979

Peter B. S. Lissaman
Bart Hibbs
Stel N. Walker
Thomas Zambrano

AeroVironment Inc.
Pasadena, California 91107

Prepared Under Subcontract
No. AH-9-8003-1
Under
Prime Contract
No. EG-77-01-4042

For the

Solar Energy Research Institute
A Division of Midwest Research Institute

1536 Cole Boulevard
Golden, Colorado 80401

COMMENT

During FY79, studies were performed by subcontractors to assess the performance and cost potential of ongoing R&D efforts in the Wind Energy Innovative Systems program. To provide a baseline for the comparison of the different studies, specifications were provided for the calculation of the cost of energy, useful service life, wind environment and maximum design wind speed.

Innovative wind systems may have operating characteristics which are different from conventional wind systems. Optimum performance and minimum cost of energy may be sensitive to wind environment and wind loads. Future assessment studies will consider the effects of these conditions on the potential of the innovative system.

Irwin E. Vas
Manager
Wind Energy Innovative
Systems Projects

FOREWARD

This report was prepared by personnel in the Aerosciences Group at AeroVironment Inc. for the Solar Energy Research Institute, Golden, Colorado, under Contract EG-77-C-01-4042, Subcontract No. AH-9-8003-1. The SERI technical monitor was Dr. Irwin E. Vas.

The report analyzes three types of horizontal axis augmented turbines. The results indicate that no augmented turbine is more cost effective than the base turbine. The most cost effective augmented system is the dynamic inducer system, followed by the ducted turbine, and lastly by the delta wing vortex augmentor.

The authors gratefully express their appreciation to Dr. Vas, who assisted in carrying out this study.

EXECUTIVE SUMMARY

A method of increasing the power output of a wind turbine is to add an augmentor system which will act like a converging duct to increase the velocity at the turbine disk and thus increase the energy flux through the power extraction device. The cost-effectiveness of such systems depends upon the trade-off between the additional energy output and the added cost of the augmentor system. The report studies the cost-effectiveness of three different types of augmentors.

A generalized augmentor theory is developed. Two common elements occur in all augmentors. These are the increased flow speed (or mass flux) through the actuator power extraction device, and the aerodynamic force on the augmentor itself, generally directed towards the axis of the actuator. Three fundamental types of augmentors are considered. Two types are passive. Of these, one has an augmentor that is a duct which surrounds the actuator (axisymmetric static); the other has an augmentor which is a delta wing in the vicinity of the actuator (planar static). The third system, a dynamic augmentor, is one in which the augmentor consists of moving airfoils (tip-vanes) attached to the rotor. Although other types of augmentors can be postulated, the above three are those for which some significant research has been conducted, thus a basis for a cost-effectiveness analysis is provided.

The ducted system has been studied by the Grumman Aerospace Corporation, the delta wing system by the Polytechnic Institute of New York, and the dynamic augmentor system by AeroVironment Inc. and the Delft Institute of Technology in Holland. For each system, both analytical and experimental studies have been made. The most comprehensive body of research has been reported on the ducted system and the least work on the dynamic augmentor. Thus, some analytical data, and supporting experimental data are available for the performance of each system, although they are not complete. This is, however, far from the case for the cost estimates, since only experimental units have ever been built of any of the systems and good cost data is not available. In fact, only for the ducted system has a power-producing test unit been built, although the components -- in particular, the augmentation systems -- have been experimentally tested for each system.

To compute the aerodynamic performance, analytical and experimental data were used for each system, using both data by developers of the system as well as values estimated in the present research. As might be expected, the developers' claims for performance were higher than those conservatively estimated in the present research and, to account for this, two performance levels were assumed. The first was called the high confidence level, being a conservative estimate which, in the opinion of the present authors, can probably be achieved. The second was called the extrapolated performance, the highest level claimed by the developers of the system. Thus, six general systems are defined.

The aerodynamic performance is summarized in Table 1, showing the characteristics of the six augmented systems and the baseline unit. Here, the power coefficient of the system ($C_{p, \text{system}}$) is defined as the power output divided by $1/2\rho V^3 A$, where ρ is the fluid density, V the wind speed, and A the swept area of the rotor. The system power coefficient gives an indication of the net amount of augmentation achieved by each arrangement. A comparison of the size and configuration of the three augmented types is given in Figure 1, which shows the relative properties of the three high confidence augmentors, with the baseline unaugmented unit at the upper right of the figure.

Table 1. CONFIGURATION POWER COEFFICIENTS

Configuration	C_P Ideal	C_P Rotor	C_P System	Ideal Augmentati Ratio
Axisymmetric, static, high confidence	2.37	1.68	1.47	4.00
Axisymmetric, static, extrapolated	4.74	3.36	2.95	8.00
Planar, static, high confidence	1.36	0.96	0.85	2.29
Planar, static, extrapolated	2.99	2.12	1.86	5.04
Dynamic, high confidence	1.56	0.71	0.63	2.63
Dynamic, extrapolated	2.00	1.02	0.90	3.37
Mod-X	0.59	0.42	0.37	1.00

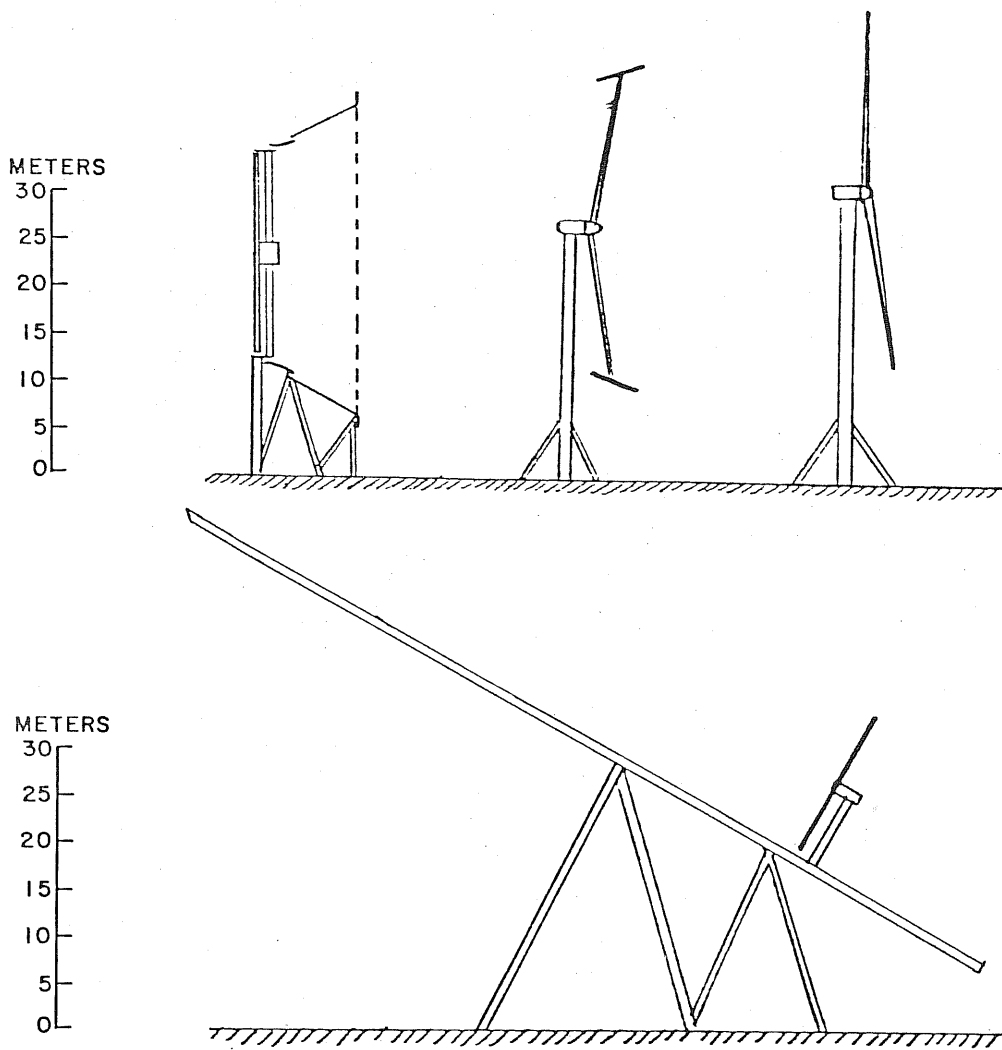


Figure 1. SKETCHES OF WIND TURBINES DESIGNED FOR THE HIGH CONFIDENCE LEVEL DESIGN

Each of these systems was then sized to produce the same performance and power output in a given wind as the NASA MOD-X wind turbine. Thus, the electrical equipment for each system will be common and of the same cost, and cost differences will lie principally in the rotor, the gear box, the augmentation system, and the tower or support arrangements. Estimates of the cost of these components were made using the known size and loads on the components and utilizing, as far as possible, the structural cost estimates provided the proponents. These are considered imprecise estimates due to the very limited experience in costing these unconventional systems for which no precedents exist, but the costing was made on a consistent basis for each machine, and all assumptions are noted.

Finally, the cost of power, in cents per kilowatt hour, for each system was calculated using a standard SERI formula involving capital cost, operations and maintenance cost, annual cost rate, and annual energy produced. The cost of power was compared with that of the MOD-X, having a cost figure of 6.3 cents/kWh for the wind duration curve specified, which has a mean wind speed of 6.04 mps (13.5 mph). These figures are shown in Table 2. In this table, the cost of a single 200 kW system of each type is shown, together with the absolute power costs and the ratio of these costs to the baseline unit. The dynamic augmentor appears the most favorable, having a power cost about 1.2 times those of the baseline MOD-X. The best extrapolated axisymmetric static system (the duct) gave a cost ratio of 1.8, the best extrapolated planar static system (the delta wing) gave this ratio as 3.0. All the augmented systems appear less cost-effective than the plain MOD-X, but it is noted that the dynamic augmentor, in spite of the very limited development devoted to it, is comparable even at its present immature level, and thus merits further attention. An outline plan of recommended future research of augmentors is given.

Table 2. SUMMARY OF CONFIGURATION COSTS

Configuration	Total Cost (Dollars)	Total Cost Ratioed to Mod-X	Cost of Electricity (¢ per kWh)	Cost of Electricity Ratioed to Mod-X
Mod-X	202,805	1.0	6.3	1.0
Axisymmetric static high confidence	600,450	3.0	16.6	2.6
Axisymmetric static, extrapolated	398,965	2.0	11.4	1.8
Planar static, high confidence	1,191,040	5.9	31.8	5.0
Planar static, extrapolated	710,150	3.5	19.4	3.0
Dynamic, high confidence	262,750	1.3	7.8	1.2
Dynamic, extrapolated	249,925	1.3	7.5	1.2

SUMMARY

A method of increasing the power output of a wind turbine is to add an augmentor system which will act like a converging duct to increase the velocity at the turbine disk and thus increase the energy flux through the power extraction device. The cost-effectiveness of such systems depends upon the trade-off between the additional energy output and the added cost of the augmentor system. The report studies the cost-effectiveness of three different types of augmentors.

A generalized augmentor theory is developed. Two common elements occur in all augmentors. These are the increased flow speed (or mass flux) through the actuator power extraction device, and the aerodynamic force on the augmentor itself, generally directed towards the axis of the actuator. Three fundamental types of augmentors are considered. Two types are passive. Of these, one has an augmentor that is a duct which surrounds the actuator (axisymmetric static); the other has an augmentor which is a delta wing in the vicinity of the actuator (planar static). The third system, a dynamic augmentor, is one in which the augmentor consists of moving airfoils (tip-vanes) attached to the rotor. Although other types of augmentors can be postulated, the above three are those for which some significant research has been conducted, thus a basis for a cost-effectiveness analysis is provided.

The ducted system has been studied by the Grumman Aerospace Corporation, the delta wing system by the Polytechnic Institute of New York, and the dynamic augmentor system by AeroVironment Inc. and the Delft Institute of Technology in Holland. For each system, both analytical and experimental studies have been made. The most comprehensive body of research has been reported on the ducted system and the least work on the dynamic augmentor. Thus, some analytical data, and supporting experimental data are available for the performance of each system, although they are not complete. This is, however, far from the case for the cost estimates, since only experimental units have ever been built of any of the systems and good cost data is not available. In fact, only for the ducted system has a power-producing test unit been built, although the components -- in particular, the augmentation systems -- have been experimentally tested for each system.

To compute the aerodynamic performance, analytical and experimental data were used for each system, using both data by developers of the system as well as values estimated in the present research. As might be expected, the developers' claims for performance were higher than those conservatively estimated in the present research and, to account for this, two performance levels were assumed. The first was called the high confidence level, being a conservative estimate which, in the opinion of the present authors, can probably be achieved. The second was called the extrapolated performance, the highest level claimed by the developers of the system. Thus, six general systems are defined.

Each of these systems was then sized to produce the same performance and power output in a given wind as the NASA MOD-X wind turbine. Thus, the electrical equipment for each system will be common and of the same cost, and cost differences will lie principally in the rotor, the gear box, the augmentation system, and the tower or support arrangements. Estimates of the cost of these components were made using the known size and loads on the components and utilizing, as far as possible, the structural cost estimates provided the proponents. These are considered imprecise estimates due to the very limited experience in costing these unconventional systems for which no precedents exist, but the costing was made on a consistent basis for each machine, and all assumptions are noted.

Finally, the cost of power, in cents per kilowatt hour, for each system was calculated using a standard SERI formula involving capital cost, operations and maintenance cost, annual cost rate, and annual energy produced. The cost of power was compared with that of the MOD-X, having a cost figure of 6.3 cents/kWh for the wind duration curve specified, which has a mean wind speed of 6.04 mps (13.5 mph). The dynamic augmentor appears the most favorable, having a power cost about 1.2 times those of the baseline MOD-X. The best extrapolated axisymmetric static system (the duct) gave a cost ratio of 1.8, the best extrapolated planar static system (the delta wing) gave this ratio as 3.0. All the augmented systems appear less cost-effective than the plain MOD-X, but it is noted that the dynamic augmentor, in spite of the very limited development devoted to it, is comparable even at its present immature level, and thus merits further attention. An outline plan of recommended future research of augmentors is given.

TABLE OF CONTENTS

	<u>Page</u>
Summary	i
List of Figures	v
List of Tables	vi
Nomenclature List	vii
1.0 Introduction	1
1.1 Axisymmetric Duct	2
1.2 Planar Wing	2
1.3 Tip-Vanes	3
2.0 Previous Work on Horizontal Rotor Systems	4
2.1 Axisymmetric Static Inducer	4
2.2 Planar Static Inducer	9
2.3 Dynamic Inducer	9
2.4 The NASA Mod-X 200 kW Wind Turbine	13
3.0 AeroVironment Generalized Performance Analysis	17
3.1 General	17
3.2 Expression for Power Coefficient	17
3.3 Effects Associated with the Brake State ($C_H > 1.0$)	20
3.4 Determination of Capacity Factor	20
3.5 System Efficiency	22
3.6 Performance of the Axisymmetric Static Inducer	23
3.7 Performance of the Planar Static Augmentor	25
3.8 Performance of the Dynamic Inducer	25
3.9 Actual System Performance	28
3.10 Rotor Sizes	30
4.0 Cost Analysis	34
4.1 Cost of Components	34
4.1.1 Rotor	34
4.1.2 Hub/Pitch Control	34
4.1.3 Bedplate and Gearbox	34
4.1.4 Electrical System	35
4.1.5 Tower	35
4.1.6 Augmentor	35
4.1.7 Foundation	36
4.1.8 Other Costs	36
4.2 System Power Costs	36
4.2.1 Mod-X	36
4.2.2 Axisymmetric Static Augmentor	36
4.2.3 Planar Static Inducer	38
4.2.4 Dynamic Inducer	38
4.3 Discussion	45

TABLE OF CONTENTS (concluded)

	<u>Page</u>
5.0 Outline of Program Plan for Further Development of Augmentor Systems	48
5.1 Summary of Augmentor Principles	48
5.2 Comparison of Systems Analyzed	50
5.3 Recommendations for Research and Development on Augmentors	51
6.0 Conclusions and Recommendations	55
7.0 References	56

LIST OF FIGURES

	<u>Page</u>	
2-1	Power Augmentation for a Ducted Rotor	7
2-2	Grumman Ducted Turbine Data	8
2-3	Tip Vane Configuration and Resulting Vortex Configuration Showing Cancellation of Tip Vane Vortices in Vortex Synchronous State	11
2-4	Augmentation of a Dynamic Inducer System	12
2-5	NASA MOD-X Baseline Configuration	14
3-1	Ideal Power Coefficient of General Augmented Wind Turbine	19
3-2	Windmill Brake State Performance for an Unaugmented Turbine	21
3-3	Pressure Amplification vs Head Loss for the Grumman Duct	24
3-4	Contours of Constant Velocity Magnitude for Vortex Field Above Basic Vortex Augmentor Surface at an Angle of Attack of 29 Degrees	26
3-5a	Vortex Augmentor in the Windmill Brake State with Successful Scavenging	27
3-5b	Vortex Augmentor with Unsuccessful Scavenging	27
3-6a	Sketches of Wind Turbines Designed for the High Confidence Level Design	32
3-6b	Sketches of Wind Turbines Designed for the Extrapolated Level Design	33

LIST OF TABLES

	<u>Page</u>	
2-1	Summary of NASA MOD-X Features	15
3-1	Configuration Power Coefficients	29
4-1	MOD-X Cost Breakdown	37
4-2	Cost Breakdown for Axisymmetric Static Inducer, High Confidence	39
4-3	Cost Breakdown for Axisymmetric Static Inducer, Extrapolated	40
4-4	Cost Breakdown for Planar Static Inducer, High Confidence	41
4-5	Cost Breakdown for Planar Static Inducer, Extrapolated	42
4-6	Cost Breakdown for Dynamic Inducer, High Confidence	43
4-7	Cost Breakdown for Dynamic Inducer, Extrapolated	44
4-8	Summary of Configuration Costs	46
4-9	C_p Based on Aerodynamic Surface Area	47

NOMENCLATURE

a	axial interference factor due to rotor
b	duct chord
B	normalized tip-vane span
c	scale parameter used in Weibull equation
C	normalized tip-vane chord
C_F	radial force coefficient
C_H	head loss coefficient
C_L	lift coefficient
C_M	mass flow coefficient
C_{M_O}	total mass flow before effects of the rotor are included
ΔC_{M_O}	increase in mass flow due to augmentor
C_P	power coefficient, $C_P = z P / \rho \pi R^2 V^3$
$C_{P_{Betz}}$	ideal power coefficient for an unaugmented wind turbine, 0.593
C_{P_L}	viscous power loss of tip-vane
C_{TL}	local disk thrust coefficient (thrust / $(1/2 \rho \pi R^2 V_{av}^2)$)
D_S	drag of the entire system
h_t	tower height
I	induction factor due to tip-vanes
k	Weibull parameter
$\Delta K.E.$	change in kinetic energy per unit mass of flow
L/D	lift to drag ratio
M	mass flow
M_a	mass flow coefficient due to turbine interference
N	number of blades on tip-vanes
p(V)	probability of wind speed over speed, V

Δp	change in pressure across rotor
P	power output
q_0	free stream dynamic pressure
q_2	dynamic pressure at the turbine disk
r	dimensionless radius
R	rotor or duct radius
R	augmentation ratio, $C_p/C_{p_{\text{Betz}}}$
T_E	equivalent downwind thrust
u^*	dimensional induced axial velocity due to tip-vanes
U	velocity at duct periphery
V	wind velocity or free stream velocity
V_{av}	average velocity through a duct
V_z	wind speed at height, z
ΔV	increase in average axial velocity due to induction
X	advance ratio of the turbine
z	height above ground
z_0	roughness height
z_r	reference height
α	normalized velocity increase through a duct
β	normalized velocity increase at a duct wall
ρ	density of air
Γ	total vorticity on duct
Γ_T	vorticity shed by tip-vane

SECTION 1.0

INTRODUCTION

A turbine provides useful work by extracting kinetic energy from the natural wind flow. Only two methods are available to increase the energy extracted. Either the amount of energy extracted from a given stream tube of the flow can be increased, or the amount of energy flux operated upon by the machine can be increased. The latter effect is accomplished by magnifying the area of the stream tube flowing through the machine. The flux magnification principle is called augmentation.

Augmentation methods can be classified into two broad categories: those that are passive and those which are dynamic or active. Passive augmentation methods involve the addition of auxiliary surfaces to the basic "free rotor" wind turbine system, designed to increase that mass flow through the actuator volume. The term "volume" is used to indicate that the actuator may occupy a finite streamwise extent. A passive augmentor will cause an increase in energy flux which can be considered as induced by a vortex system. This vorticity is coupled with the axial flow to produce an inwards force on the system. The reaction to this effect is an outward force on the stream tube which causes it to diffuse downstream, thereby increasing the stream tube capture area.

Two techniques of passive augmentation are considered in this report. The first is an axisymmetric duct. For such a system, the duct ring vorticity is coupled with the axial flow to produce a radially-inwards force on the duct. The reaction to this effect is a radial outward force on the stream tube. The second passive augmentor is a planar wing. The power extracting device in this system is located above the suction side of the wing, where the flow speed has been increased by the wing bound vorticity. The augmentation here is not due to the swirl of the vortex, which cannot increase the net energy flux of the flow, but is actually due to the greatly increased axial flow speed which causes an increased mass flow through the actuator (Loth, 1977). Again, a force towards the actuator must be developed. In this case it is the lift on the wing. Thus we see that the wing performs a function similar to the duct.

One feature of all passive augmentation devices is that, because they do not move relative to some inertial axis, they can do no work on the flow and thus do not require any additional energy to operate. In fact, the duct and the planar wing experience large streamwise drag-like forces. It is this dragwise force (in addition to the dragwise force on this actuator) which couples with the effective streamwise velocity at the machine to produce the power extraction. Considering the system in the global sense, an equation of the type $P = D V_e$ can be written to define the power, P , extracted from the wind stream, where D is the total windwise drag of the system and V_e the effective windwise flow through the actuator.

The other major class of augmentation is achieved through what can be described as dynamic augmentation. In this case, elements moving relative to an inertial axis are used to create an increased flow through the actuator, accompanied by a cross-stream force directed towards the axis of airstream from which the energy is extracted. The technique of dynamic augmentation considered in this report is a tip-vaned rotor system.

The tip-vane rotor system, called the Dynamic Inducer, when applied to a propeller-type actuator, may be likened to a static duct where the radial force is developed by vanes on the tips of the power rotor (the propeller). The tip-vanes are set to develop a radially-inwards force which produces a slip stream expansion comparable to that caused by a

duct. However, the effective dynamic pressure of the tip-vanes is proportional to X^2 times the dynamic pressure of the free stream flow, where X is the tip speed ratio. Thus, significantly less area of tip-vane is needed to produce the same radial force that the duct can generate.

Although the dynamic induction system can produce flow augmentation with additional lifting surface elements significantly lower than static inducers, it must be noted that the dynamic inducer vanes in general do work on the flow and thus require power to operate. The net effect must be obtained by subtracting the power required to drive the induction system from the power produced by the power vanes. It has been shown that the power consists of two components, that due to viscous drag of the inducer vanes and that due to their induced drag. The first component is unavoidable, but can be minimized by using a system of low profile drag. The latter component is a function of the precise geometry of the helical vortex system shed by the inducers.

The scope of this report is to investigate the three described wind energy augmented systems. Specifically this report includes a technical evaluation of the most up-to-date work in this field, and assesses the horizontal axis rotor systems performance and cost-effectiveness in relation to the NASA Mod-X 200 kw free rotor wind turbine concept. The three augmented systems performance analysis will be based on the following published reports.

1.1 AXISYMMETRIC DUCT

Grumman Aerospace Company has put considerable effort, during the past four years, into developing a short, cost-effective diffuser for wind energy conversion applications. The major effort has been experimental, with theoretical guidance provided by a one-dimensional baseline diffuser configuration. Combined with a working but not optimized turbine, wind tunnel tests conducted by Grumman have reported the ability of a ducted turbine to produce almost 3.5 times the ideal power coefficient of a conventional wind turbine of the same size. This power coefficient is computed from the downstream force on the rotor, the stream velocity, and the rotor area. Grumman's projections of these data to their optimum turbine load factors and operating speed ratio conditions result in power coefficient levels over eight times those of the best conventional wind turbine. Grumman has also supplied a parametric cost breakdown of their ducted rotor system. The work is described in the draft final report on Further Investigations of Diffuser Augmented Wind Turbines (Foreman, 1978; Gilbert, 1978).

Grumman's performance analysis will be compared to an AV-developed ducted rotor analysis. AV has developed a generalized analysis of the performance of rotors in ducts, taking into account the multi-energy flow in the wake and the energy extraction due to the actuator. This analysis exhibits the effects of duct divergence angle and duct camber.

1.2 PLANAR WING

The Polytechnic Institute of New York Aerodynamic Laboratories has devoted much effort into a vortex augmentor concept employing a low aspect ratio delta platform. Flow separated in the form of leading edge vortices from highly swept sharp leading edges concentrates the kinetic energy density of the wind from a large upstream area into a kinetic energy density flow in a small vortex area. Sforza and Stasi (1978) report that the interaction between a fluid stream and a suitably designed aerodynamic surface can provide regions of kinetic energy density up to nine times that of the free stream kinetic

energy density. Sforza's predictions of rotor performance of a delta wing system suggest a four-fold increase in power over unaugmented operation. Cost analysis is made through a parameter approach developed by AV. The work on this system is described in reports from the New York Polytechnic University on Vortex Augmentors for Wind Energy Conversion.

1.3 TIP-VANES

AeroVironment has been actively engaged in the development of the dynamic inducer rotor (DIR) concept for several years. A complementary program on the DIR is being conducted at the Delft Institute of Technology under the directorship of Dr. Theodore van Holten (van Holten, 1978). The DIR concept has the theoretical potential of increasing the power output of wind turbines by a factor of 2. The principle involves increasing the flow velocity through the actuator volume by means of moving airfoils attached to the rotor system, thus dynamically inducing a higher mass flux from which more energy can be extracted. The key results of the Delft team, reported in van Holten (1977), have been that substantial induction can be achieved from the tip-vanes. This induction has been determined in flow visualization tests by measuring the radius of a smoke filament striking at the tip-vane radius and comparing this with the case of no tip-vanes. Up to four times the normal mass flow has been achieved with the induction effect. As the induction is caused by the axial force generated by the tip-vanes, measuring this induction allows direct determination of the axial force. The axial force has not been directly measured, however.

The analytical work at Delft has involved computation of flow fields using a method of asymptotic approximation and, as such, constitutes a different mathematical approach from the vortex methods employed by AeroVironment. Close collaboration exists between AV and Delft, and it is found that the predictive methods developed by both organizations correlate and support each other. The work on this system is described in technical reports to the DOE by AV (Lissaman and Walker, 1978) and memoranda on tip-vanes by Delft University of Technology (van Holten, 1974-1978).

Section 2 will present a detailed summary of previous analytical work that has been accomplished on three types of augmenting systems, as well as a summary of the general features for the selected baseline NASA Mod-X configuration. Section 3 will present the AV Generalized Performance Theory which will be used to evaluate and extend the analysis for each of the three augmented systems. Cost models will be made with reference to the NASA Mod-X system and reported in Section 4. Section 5 will discuss future research and development efforts necessary to practically apply these concepts to technology, and also summarize the cost-effective potential and limitations of each system.

SECTION 2.0

PREVIOUS WORK ON HORIZONTAL ROTOR SYSTEMS

The past work on the design analysis and the performance of the three augmented systems and the free rotor baseline system are evaluated in this chapter. The first section summarizes previous analytical work (Grumman, Sforza, AV) that has been accomplished on the three types of wind machines. The second section summarizes the NASA Mod-X free rotor turbine performance and characteristics. This chapter is followed by an AeroVironment generalized performance analysis which extends the previously described linear theory into the windmill brake state. The results of this extended analysis is that for each of the three systems, two design augmentation ratios are rationally selected. One design will reflect what AV evaluates to be a "high confidence" limit; the second design will be the most optimistic limit which has been published or conveyed to AV by private communication from the sources consulted.

The aerodynamic performance of each system must be defined in terms of power versus tip speed ratio so that the effects of cut-in and cut-out speeds, rated speeds, power output range, and power factors can be examined. Based on the specific performance parameters of the NASA Mod-X, and the velocity duration profile specified by SERI, the capacity factor will be determined from an AV-developed computer program and used as the standard of comparison for each of the augmented systems.

The performance parameters of each energy system are then evaluated in terms of the wind turbine subsystems: turbine support structure, yaw control, generator, speed controls, hub, rotor, augmenting device. Weight data is required for the wind turbine subsystems for costing purposes.

2.1 AXISYMMETRIC STATIC INDUCER

A theoretical analysis developed by AeroVironment (1977) of the typical static inducer, a cylindrical duct, provides some insights into the power amplification. Assume that the total vorticity on a chordwise section is Γ , it can then be shown that the mean value ΔV of the velocity induced through the duct is given by:

$$\Delta V = \Gamma\alpha/R . \quad (2-1)$$

While the velocity at the duct periphery is given by

$$\Delta V = \Gamma\beta/R . \quad (2-2)$$

Expressions for α and β for elliptical loading on the duct surface (van Holten, 1974)

$$\alpha = \frac{1}{\pi} \left[\ln(4R/b) + 1/2 \right] . \quad (2-3)$$

$$\beta = \frac{1}{4\pi} \left[\ln(32R/b) - 5/16 \right] . \quad (2-4)$$

where R is the mean radius of the duct and b is the chord. Elliptical loading was chosen by van Holten for computational simplicity. Other loadings are possible. The mass flow through an area can be referenced by the mass flow coefficient, C_M . The definition of C_M is

$$C_M = \frac{M}{\rho \pi R^2 V_{av}} , \quad (2-5)$$

where M is the mass flow rate through a circle of radius, R . The average flow velocity is V_{av} .

The additional mass flow coefficient induced by the circulation about duct, ΔC_{M_O} , may be expressed as

$$\Delta C_{M_O} = \frac{\alpha \Gamma}{VR} , \quad (2-6)$$

while the total wake mass flow coefficient, C_{M_O} , is given as

$$C_{M_O} = (1 - a) + \Delta C_{M_O} , \quad (2-7)$$

where a is the axial interference factor, and will be underlined in the text for clarity.

The energy extracted per unit mass in the wake, $\Delta K.E.$, is

$$\Delta K.E. = 2a (1 - a) V^2 . \quad (2-8)$$

Therefore, using the above relations, the total power may be expressed as

$$P = \rho \pi R^2 V \left[\Delta C_{M_O} + (1 - a) \right] 2a (1 - a) V^2 . \quad (2-9)$$

The power coefficient, C_P , based on rotor area is given by

$$C_P = 4a (1 - a) \left[\Delta C_{M_O} + (1 - a) \right] . \quad (2-10)$$

Now assuming $a = 1/3$, as is typical of unaugmented wind turbines, then

$$C_P \simeq 16/27 + 8/9 \Delta C_{M_O} . \quad (2-11)$$

The increased power can be physically explained by the radially inward force system on the shroud. This force system imposes a radially outward force on the flow in the vicinity of the actuator, forcing divergence and an increased stream tube area in the wake, and convergence, with increased flow near the entrance of the duct.

Expressing the radial force on the duct in terms of the duct radial force coefficient, C_F ,

$$\rho U \Gamma = 1/2 \rho U^2 C_F b , \quad (2-12)$$

where U is the mean velocity at the duct periphery, given by

$$U = V (1 - a) + \beta \Gamma / R . \quad (2-13)$$

Therefore,

$$\Gamma = \left[V(1 - a) + \beta \Gamma / R \right] b/2 C_F . \quad (2-14)$$

Noting that $\Delta C_{M_0} = \alpha \Gamma / V R$, and ignoring the $\beta \Gamma / R$ term (which is of the order of 0.1), the ratio of the power coefficient to the Betz power coefficient (16/27) is now expressible to the first order in Γ , as

$$\frac{C_P}{C_{P_{\text{Betz}}}} = 1 + \alpha C_F \frac{b}{2R} . \quad (2-15)$$

Figure 2-1 shows the approximate power augmentation variation with C_F and b/R for typical ducts. A more flexible representational analytical model of a duct would assume a duct shape rather than a vorticity distribution. This refinement is currently being developed by AV.

Many compact diffuser configurations have been evaluated by the Grumman Aerospace Corporation using about 150 test models of different sizes and geometry. The most promising compact diffuser emerging from this work employs slot-injected external air to prevent core flow separation and a trailing edge flap for rapid divergence or dumping of the flow from the boundary layer controlled diffuser. The Grumman DUMP diffuser design features are proprietary, however the basic specifications feature an included angle of 60 degrees, a length-to-inlet diameter ratio of 0.4 and an area ratio (the ratio of the exit to inlet area) of 2.78.

Grumman ran extensive wind tunnel tests for several turbine models. Figure 2-2 (supplied by Grumman) shows augmentation ratio, \hat{R} , versus disk loading for several ducted turbines. Peak augmentation ratio obtained for the near-unity speed ratio is 3.4 when referenced to the Betz limit for free turbines. Grumman reported that if their Baseline diffuser (note: the Grumman DUMP diffuser is a more recent generation design than the described Grumman Baseline diffuser) had been able to operate at a tip speed ratio of 5 or 6, which compares to a characteristic tip speed ratio of 9.4 for the NASA Mod-X wind turbine, instead of the actual 1.09, the greater turbine efficiency accompanying the higher speed ratio would have raised the expected augmentation ratio to almost 4.7 at a disk loading of about 0.4. Furthermore, Grumman argued that because overall augmentation ratio,

$$\hat{R} = \frac{C_{TL}}{.593} (q_2/q_0)^{3/2} , \quad (2-16)$$

where q_2/q_0 is the ratio of dynamic pressure at the upstream face of the turbine to that of the freestream, and C_{TL} is the local disk loading, the peak augmentation ratio based on the trend shown in Figure 2-2 would be predicted to occur at a local disk loading of about 0.9 and reach a value of 6.3. Grumman added that diffuser designs that provide "refinements" to the initial baseline configuration bring expected peak augmentation ratio values above 7.0 for efficient operating turbines. For the Grumman DUMP diffuser Grumman predicts that at a disk loading of 2.07, the peak augmentation ratio will reach a value of about 8 (Foreman, 1979). These predictions are based on extrapolations from data made with the non-optimum rotor.

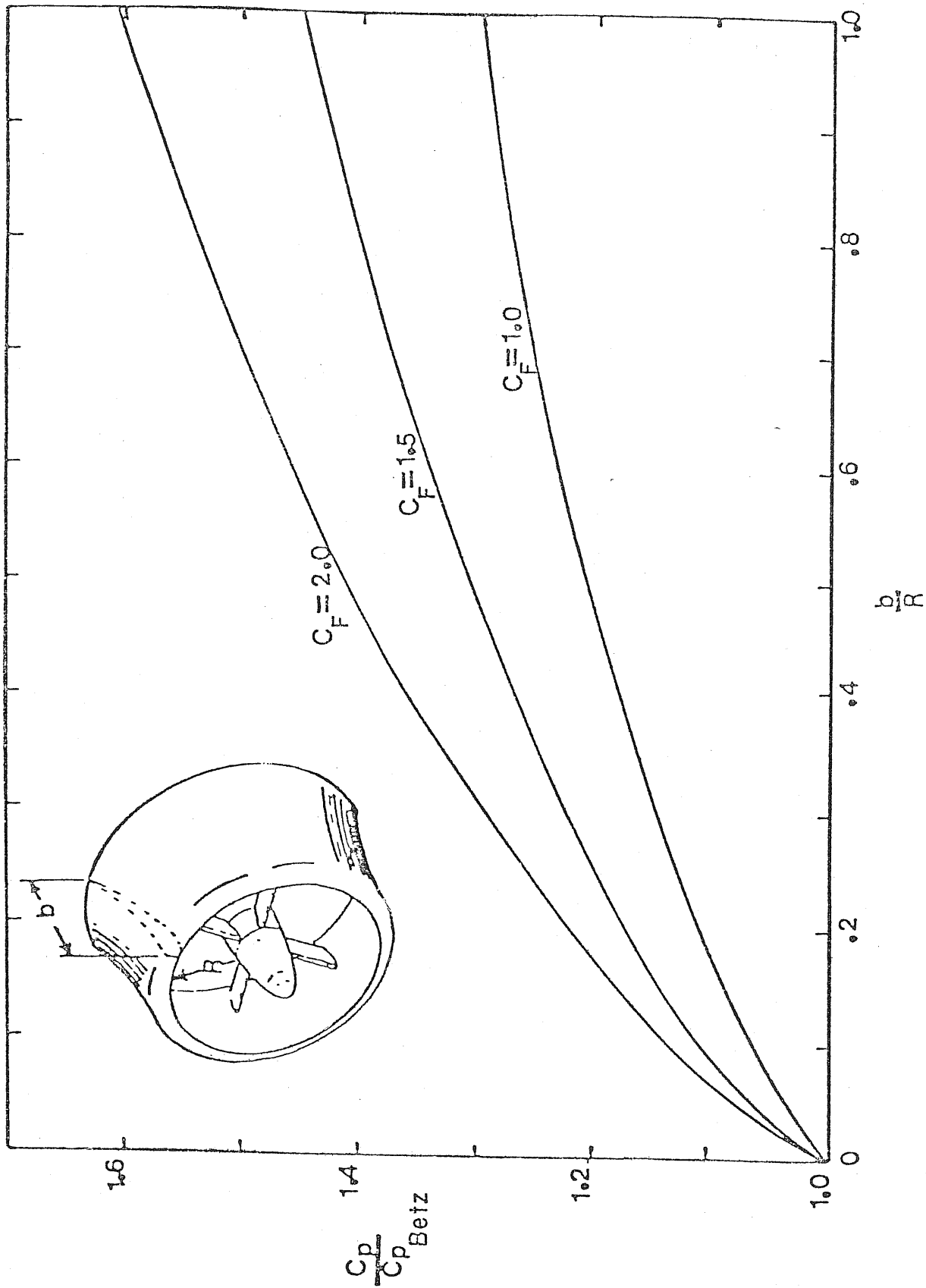


Figure 2-1. POWER AUGMENTATION FOR A DUCTED ROTOR

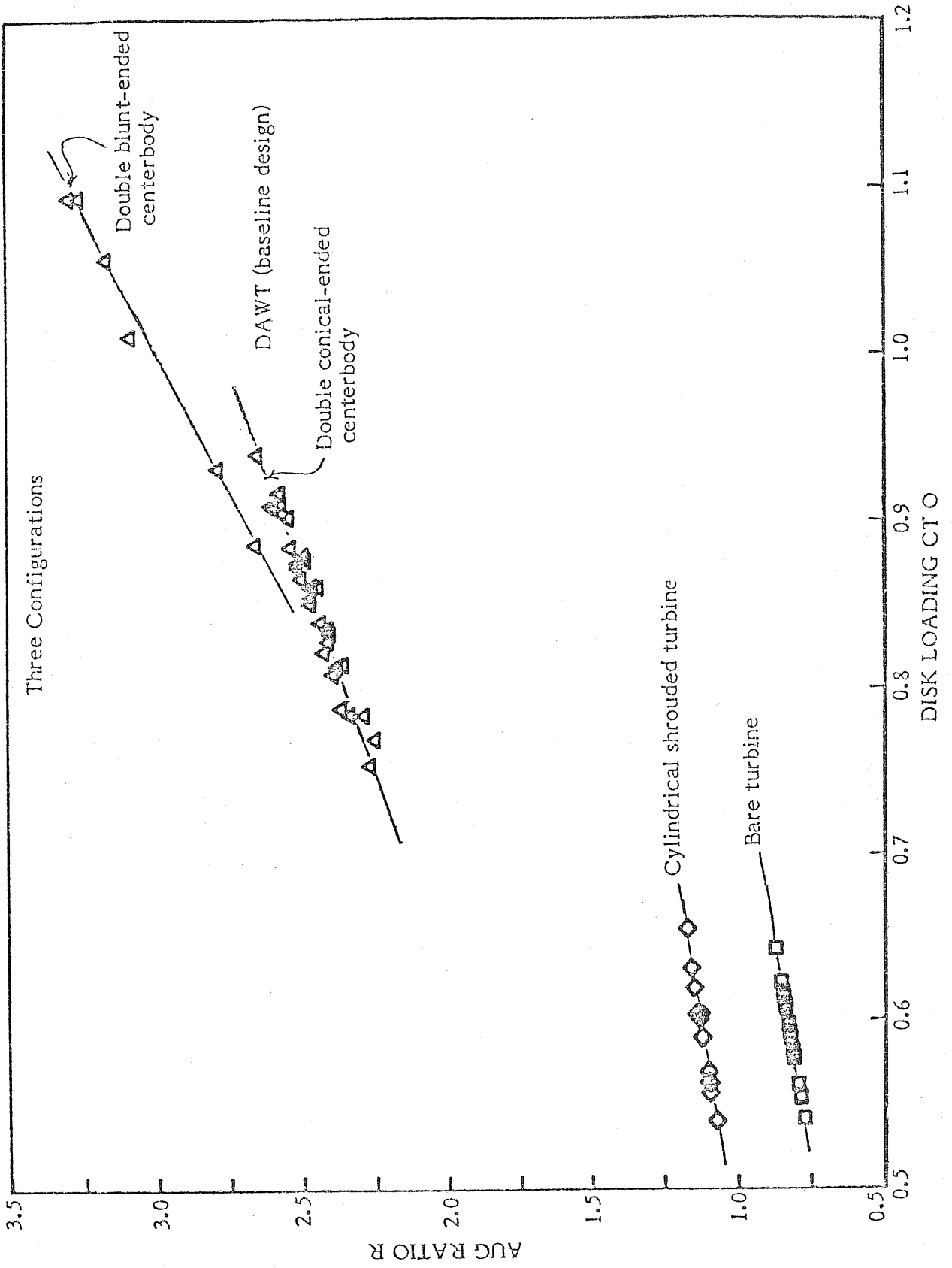


Figure 2-2. GRUMMAN DUCTED TURBINE DATA

2.2 PLANAR STATIC INDUCER

In "conventional" wind turbine design, the power extracted is controlled by alteration of the pitch of the rotating blade at the hub, where the stresses are the greatest. A planar wing surface (called a vortex augmentor), "pre-processes" the natural wind and generates a particular power distribution above the upper surface.

Experiments conducted at the Polytechnic Institute of New York (PINY) by Sforza and Stasi indicate that the power level and its distribution depend upon planform shape and angle of attack. Also, changes in camber, such as produced by deflection of a trailing edge flap, can affect the power level and distribution above the augmentor surface. A variation of ± 15 degrees in flap direction, for example, experimentally resulted in a change in available kinetic energy by a factor of 2.5 between the two extremes in flap deflection.

Sforza interprets the augmentation to result from the following logic. The vortex flow field has a swirling character; therefore, a turbine placed in the flow can be made to rotate in the same sense as the vortex. Rotation with the vortex allows turbine rotation at a much higher tip speed ratio. The planar surface is thereby viewed by Sforza to act as a "pre-rotation vane" (Sforza, 1976).

This may be a misleading explanation of the flow augmentation mechanics. The additional velocity component induced by the swirl in the radial direction is secondary compared to the greatly increased axial flow velocity which results from the angle of incidence of the planar surface. Furthermore, the swirl of the vortex cannot increase the net energy flux of the flow but, in fact, can generate irreversible energy losses due to viscous effects. Once again, it is an increased mass flow through the actuator which causes the flow augmentation.

Sforza reports experimental results for the case of uniform upstream flow in a rotor test facility designed at PINY. The delta used was 2.18 meters long and was set at various angles of attack. For the case when the rotor is immersed in the vortex of a flat plate delta at an angle of attack of 25° , the maximum power generated by the rotor is approximately four times that of the unaugmented rotor (Sforza, 1976). These values may not be representative of the amount of power augmentation possible. This is because a rotor optimized for use in the vortex flow field was used for the free rotor tests. Thus, the power level for the unaugmented rotor may be lower than is feasible, resulting in a higher than justified augmentation ratio being reported.

The adequacy of these laboratory experiments is currently under investigation in field trials of a prototype system. The prototype is a simple flat plate delta 6 meters long with a 75° leading edge sweepback set at an angle of attack of 29° .

2.3 DYNAMIC INDUCER

The AV duct theory previously described has shown that a radially outward force exerted on the air near the actuator can have a very advantageous effect. The radial force creates the increased mass flow through the disk, and consequently the large diffusion. This required radial force can be created very effectively by tip-vanes.

Since the tip-vanes are moving at tip speed, their effective dynamic pressure is proportional to the square of the tip speed ratio, X . Thus, the tip-vanes can produce the same radial force as a static duct, with a very much smaller surface area. In comparison,

for the same diffusion and force coefficient, the ratio of tip-vane area to duct area varies as $1/X^2$, a very significant reduction in area, since X is typically about 10.

Another important difference exists between the dynamic inducer (tip-vanes) and the static inducer (cylindrical duct). Tip-vanes are attached to the blades, and thus drag forces on the tip-vanes represent power losses. The drag may be of two types -- induced and profile. The profile drag can be readily computed and converted to a viscous power coefficient loss, C_{PL} (Lissaman, 1978).

$$C_{PL} = \frac{1}{\pi} X^3 C_B \frac{C_L N}{L/D} , \quad (2-17)$$

where

- B = Span of tip-vane (normalized by radius)
- C = Chord of tip-vane (normalized by radius)
- N = Number of tip-vanes
- C_L = Force coefficient of tip-vane
- L/D = Lift/drag ratio of tip-vane airfoil section

The induced drag of the tip-vanes is caused by the vorticity shed from the tip-vanes. Any lifting surface sheds vorticity from its tips. The tip-vane vortex system can be modeled as a wing shedding vorticity at its tips, thus creating two trailing vortex lines or filaments -- in this case, N wings shedding vorticity. If the span of the tip-vane $B = 2\pi/NX$, then, assuming a horseshoe vortex, the trailing vortex of the upwind tip of one tip-vane goes through the downwind tip of the succeeding tip-vane. The vortex shed by the downwind tip of the tip-vane is of equal magnitude, but opposite sign from the upwind tip, causing the vortex to be exactly cancelled. Nonuniform flow will upset this process, but the magnitude of the departure from perfect cancelling is expected to be small when future measurements are made. It is noted that this vortex cancelling effect has been observed by van Holten (1978), along with the elimination of induced drag. Figure 2-3 shows the path of the vortex filaments from the tip-vane tips. In this optimum case, a saw tooth ring vortex is produced in which there is no radial flow or shed vorticity (Lissaman, 1978). Since there is no shed vorticity, the induced drag must be zero.

The total power augmentation for tip-vanes, including viscous losses, can now be expressed as (Lissaman, 1978):

$$\frac{C_P}{C_{P_{Betz}}} = 1 + (3X/8\pi) I C C_L \left(1 - \frac{9X}{L/D I} \right) , \quad (2-18)$$

where

$$I = f(N, X) = \frac{4\pi R}{\Gamma} \int_0^1 u^* r dr , \quad (2-19)$$

u^* = dimensional induced axial velocity due to tip-vanes

r = dimensionless radius

This expression is plotted in Figure 2-4 and shows that power augmentation increases of 50% are attainable at optimal conditions for relatively small tip-vanes.

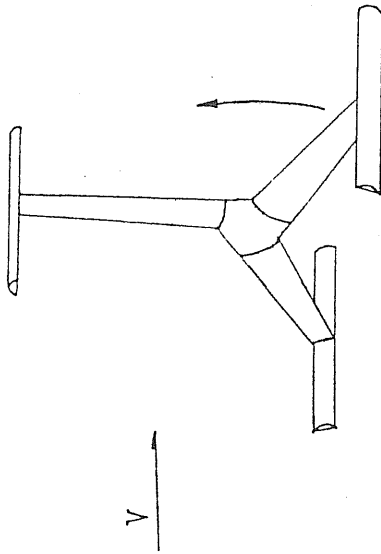
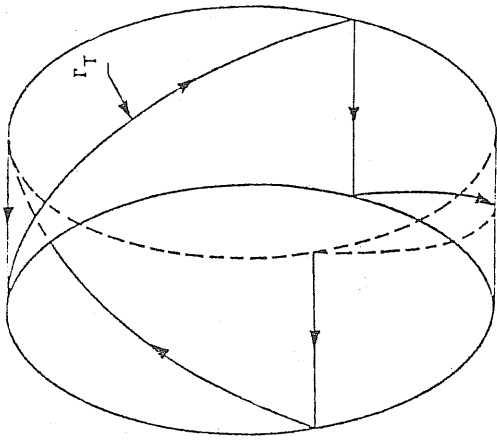


Figure 2-3. TIP VANE CONFIGURATION AND RESULTING VORTEX CONFIGURATION SHOWING CANCELLATION OF TIP VANE TIP VORTICES IN VORTEX SYNCHRONOUS STATE

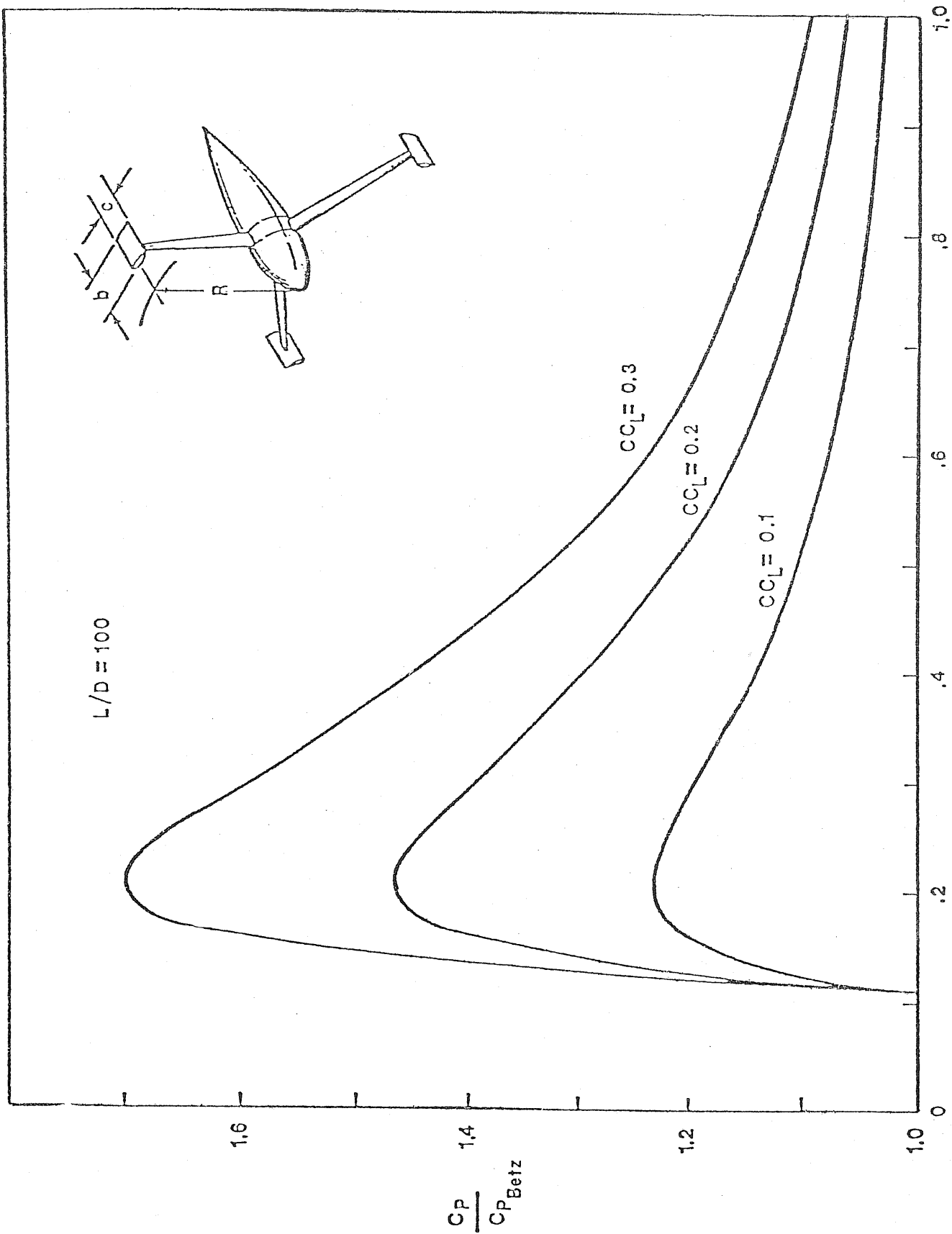


Figure 2-4. AUGMENTATION OF A DYNAMIC INDUCER SYSTEM

2.4 THE NASA MOD-X 200 kW WIND TURBINE

The NASA baseline Mod-X configuration was the result of an intensive evaluation and trade-off study of major components and subsystems (NASA, 1979). NASA's selection of the baseline configuration was guided by the philosophy that those features of a wind turbine that were shown to be potentially cost-effective and to be technically feasible in earlier NASA work were to be incorporated into the Mod-X baseline configuration and changed only if proven to be too costly or impractical during the design.

Efforts to reduce the weights and costs were made on all components and subsystems, with special emphasis on the major subsystems: the rotor, drive train, yaw drive, tower and installation. A sketch of the Mod-X baseline configuration is shown in Figure 2-5. Table 2-1 is a list of the Mod-X features.

The pod assembly consists of all the equipment atop the tower (rotor, gearbox, pitch control, etc.). The pod assembly used in the Mod-X consists of a rotor mounted directly on a low-speed shaft of the gearbox and a generator bolted onto the gearbox casing at the high speed shaft. This type of assembly was developed in the NASA Mod-1A study. The compactness and cost savings are achievable because gearbox manufacturers routinely build combinations of gearboxes and generators for a variety of large industrial applications. Several gearbox suppliers indicate that it would be a straightforward matter to design and mass produce systems that would include a gearbox, a generator, a yaw bearing, and other needed auxiliary equipment at costs less than those of the individual components. With the gearbox functioning as the main supporting structure for the generator, pitch change mechanism, and rotor, the bedplate is either eliminated or greatly reduced in size and weight. Combining the generator, gearbox, yaw bearing, rotor hub, and other components into a single factory-assembled package also reduces both fabrication costs and field assembly costs.

The hub should be designed for low weight and ease of fabrication. The hub structure must be designed to carry blade loads to the low speed shaft and be designed for adequate fatigue life. It must interface with the blades and the low speed shaft. The hub allows the blades to teeter, and provides for passage and support of the pitch drive mechanism. The hub requires provision for a teeter damper, and extreme teeter angle stops.

The blades must be designed for two loading conditions. First, they must withstand a wide spectrum of relatively low loads during operation that can cause cumulative fatigue damage. Second, they must withstand high loads that occur infrequently, such as a hurricane wind load. Low blade weight is also a desirable feature. An airfoil should be selected to provide good aerodynamic performance, allow ease of fabrication, and allow for adequate structural design.

In the NASA Mod-X study, the structure of the various blade concepts that were considered was sized using wind loads for a steady 150 mph wind at hub height. In addition, the blade structure was chosen so that the natural bending frequencies were above 2 per revolution and were not some integer multiple of the rotor rpm. NASA did not select a final blade design and material because there was no obvious choice of a blade design that would provide a significant cost reduction and would withstand the rigors of wind turbine operation. Several concepts now under development were considered as candidates for the Mod-X. These include a wood blade, a steel spar and rib blade, a steel blade, and a transverse fiberglass tape (TFT) blade.

The basic pitch change mechanism (PCM) for the Mod-X would consist of a linear actuator that is located on the rotor axis with a push rod inside the rotor shaft, and a pair

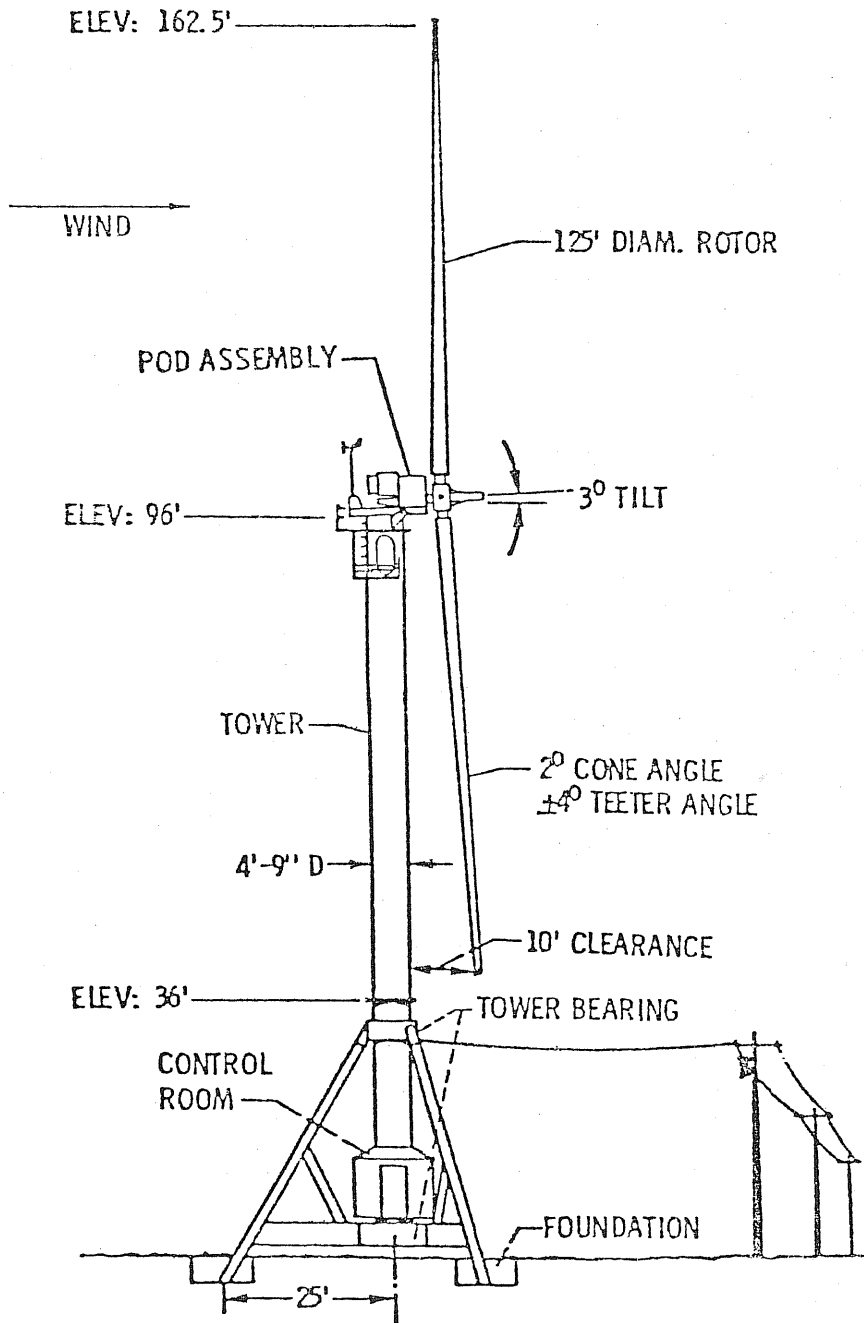


Figure 2-5. NASA MOD-X BASELINE CONFIGURATION

Table 2-1. SUMMARY OF NASA MOD-X FEATURES

- Rated power - 200 kW
- Rotor
 - Two blades, 125-foot diameter downwind
 - Teetered hub
 - Hub height - 100 feet
 - Rpm and power control - pitchable blades (either partial or full span)
 - Mount on low speed shaft of gearbox
- Gearbox - 3-stage, parallel shaft
- Alternator
 - 200 kW, 1800 rpm
- Yaw drive - passive
- Control/safety system - microprocessor based on system capable of handling all control and safety functions for unattended automatic operation
- Tower - cantilever rotating cylinder
- Foundation - factory precast concrete vaults - dirt-filled

Source: NASA, 1978

of straight links that connect the end of the rod to a bell crank at the root of each blade. This system converts the linear motion and force of the actuator to the rotary motion and torque needed to pitch the blades. Around the actuator rod is a large coil spring whose function is to supply power to quickly feather the blades during an emergency shutdown.

The gearbox functions include supporting the rotor on the input shaft, incorporating the generator as an integral structure on the high speed shaft side, and housing the yaw gear. To be able to carry the added loads, the gearbox casing, the input shaft, and the bearings would have to be heavier than usual. The added weight of the gearbox would be offset by a greater weight and cost reduction that resulted from elimination of both the large bedplate and the separate rotor main shaft and its bearings.

The Mod-X tower would be made of cylindrical members, have vertical loads transmitted into three legs by a bearing at the 35-foot elevation level, and have the horizontal loads resisted by bearings at the 35-foot elevation and at ground level. The foundation would use precast concrete vaults backfilled with excavated earth. Tower sections would be fabricated with all the necessary electrical wiring, hydraulic lines, and other equipment preassembled at the factory. Placing the rotating/stationary interface at the tower base reduces the amount of equipment that must be on top of the tower and, therefore, decreases maintenance costs. The design provides for easy installation and eliminates the need for a large crane. Rotating the tower mass provides greater stability for possible yaw, and access to the top of the tower is protected from the elements.

Further design specifications can be obtained from the NASA "200 kW Wind Turbine Generator Conceptual Design Study" (1979). Using the weights of the major components for the Mod-X subsystems, costs were determined by NASA using a dollars-per-pound figure chosen from available data for mature mass-produced products. The complete cost breakdown will be discussed in Section 4.

SECTION 3.0

AEROENVIRONMENT GENERALIZED PERFORMANCE ANALYSIS

3.1 GENERAL

In this chapter the system performances of the Axisymmetric Static Inducer, the Planar Static Augmentor, and the Dynamic Inducer are determined. For each system, two sets of performance parameters are calculated. The first set is called the "AV high confidence" parameters. These reflect what AV believes to be the most realistic values based on the AV generalized performance analyses. The second set of parameters is called the "extrapolated" set. The values in this set are based on the most optimistic performance numbers, published in the literature by the organizations which are involved in the design and development of each augmented system accordingly.

The scope of this chapter is to first derive the expressions for power in the inviscid case, then apply system efficiencies to obtain actual performance coefficients. From this, the configuration power coefficients and rotor sizes for the "high confidence" and "extrapolated" case of each of the three augmented systems are obtained.

3.2 EXPRESSION FOR POWER COEFFICIENT

In the inviscid case, the amount of power produced by a wind turbine is equal to the amount of energy removed from each unit mass of air times the amount of mass flowing through the rotor. The amount of power removed from each unit mass is proportional to the head loss, and it can be normalized to get the head loss coefficient, C_H , by dividing by the free stream dynamic pressure, q .

$$C_H = \frac{\text{Head loss}}{q} . \quad (3-1)$$

The only way fluid can lose head when flowing through a planar actuator disc is by a pressure drop, ΔP . This would have $C_H = \Delta P/q$. The definition of the thrust coefficient is:

$$C_T = \frac{\text{Thrust}}{qA} = \frac{\Delta p A}{qA} = \frac{\Delta p}{q} . \quad (3-2)$$

Thus, the thrust coefficient is equal to C_H .

The mass flow can also be normalized by the rotor area, A , and the free stream velocity to get the mass flow coefficient, C_M .

$$C_M = \frac{\text{Mass flow}}{VA} . \quad (3-3)$$

We can now get the power coefficient, C_P .

$$C_P = \frac{(\text{Mass flow}) (\text{Head loss})}{qVA} = C_H C_M , \quad (3-4)$$

C_H can be found from the axial interference factor, \underline{a} , using momentum theory (Wilson, 1976).

$$C_H = 4a(1 - a), \quad (3-5)$$

or

$$a = \frac{1 - \sqrt{1 - C_H}}{2}. \quad (3-6)$$

Momentum theory for an inviscid flow states that C_H can never exceed one. A C_H greater than one indicates that more energy is being C_H extracted from the flow than is contained in the flow. This is apparently impossible; however, methods and effects of exceeding a C_H of one by various viscous or turbulent processes will be discussed below.

Finding the mass flow coefficient is somewhat more complicated. Basically, C_M can be broken down into two components. The first is the mass flow caused by the augmentation device. This is called the no load augmentation, C_{M_0} . The second component is the decrease in mass flow due to the turbine. This component is proportional to \underline{a} , with the proportionality constant being M_a , the mass flow loss coefficient due to axial interference. Thus, the mass flow coefficient is:

$$C_M = C_{M_0} - M_a a. \quad (3-7)$$

The values of C_{M_0} and M_a are dependent upon the geometry of the system. For a free rotor, they are both equal to one. Putting this into the equation for C_P ,

$$C_P = 4a(1 - a)(C_{M_0} - M_a a), \quad (3-8)$$

we get the familiar relation for the C_P of a free turbine,

$$C_P = 4a(1 - a)^2, \quad (3-9)$$

which has a maximum of 0.593 when \underline{a} is one-third. The power coefficient equation can be optimized for any set of values for C_{M_0} and M_a by choosing the correct \underline{a} . This has been done in Figure 3-1 for the particular cases of M_a of one and two, and a range of C_{M_0} . If C_{M_0} and M_a are known, this figure allows the power coefficient to be determined in a quick and simple manner. C_{M_0} can be found either theoretically or experimentally, and M_a of one is typical of a system with a free rotor. A value of 2 is typical for a ducted system.

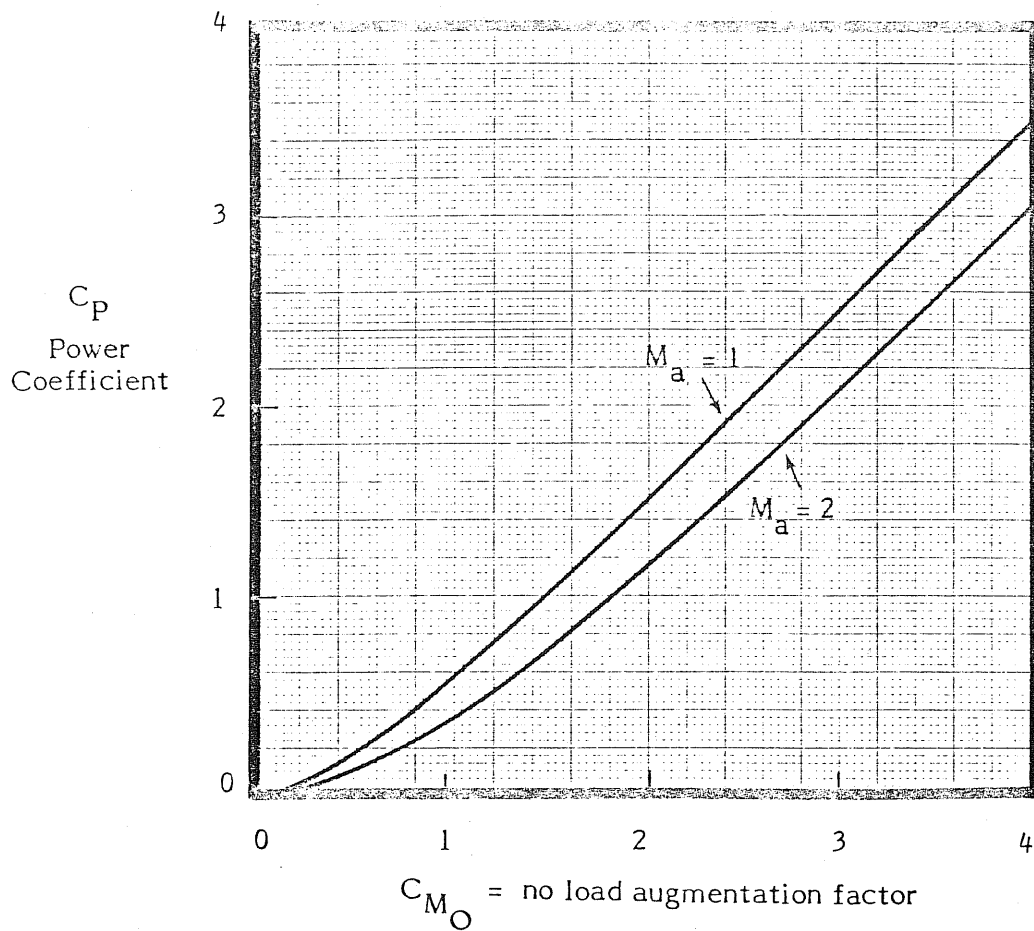


Figure 3-1. IDEAL POWER COEFFICIENT OF GENERAL AUGMENTED WIND TURBINE

3.3 EFFECTS ASSOCIATED WITH THE BRAKE STATE ($C_H > 1.0$)

An augmentation device only increases the mass flow through the actuator volume. It does not increase the energy content of a unit mass of flow. Although an augmentation system can increase the kinetic energy of the flow, the pressure of the flow will decrease, thus keeping the total energy (or head) of the flow the same. This is confirmed by the Bernoulli equation. The coefficient C_H is a measure of what fraction of this available energy is removed from the flow. Thus, it would appear that a C_H greater than one is impossible. However, data on normal windmills indicate that values up to a C_H of two have been achieved. This has been shown experimentally in Figure 3-2.

A windmill operating with a C_H greater than one is said to be operating in the windmill brake state. This state has a number of interesting characteristics. First, the axial interference factor, \underline{a} , is greater than 0.5. According to momentum theory, this would cause the flow in the wake to reverse and proceed upstream. In real turbines, there is indeed reversed flow regions in the wake (Wilson, 1976). There is also turbulence and unsteady flow processes. The actual flow field has not been determined.

Any windmill operating in the brake state is removing more energy from the flow than is contained in the flow in the captured streamtube. This can only occur if there is some process for adding energy to this flow. It is suggested here that this energy comes from outer flow turbulently mixing with the wake flow. This process produces a scavenging effect that removes the de-energized wake flow from the vicinity of the turbine. If this did not occur, the wake material would create a large reverse flow region that would prevent additional flow through the turbine and prevent operation in the brake state. Thus, the scavenging effect indirectly allows the turbine to remove energy from flow that does not pass through the turbine. However, even when this extra energy is considered, the power coefficient of a normal windmill is still lower when in the brake state than when not in it. For an augmented system, however, the reverse may be true. In fact, data from the Grumman ducted turbine tests indicate that the maximum power point may lie deep in the windmill brake state. In order to determine the maximum possible C_P for an augmented system, it is necessary to develop a theory for the windmill brake state. At the present time there is only an empirical theory for free turbines and none at all for augmented systems. In order to find what is needed of such a theory it is necessary to again consider the basic equation for C_P .

$$C_P = C_H C_M = C_H (C_{M_O} - M_a \underline{a}) . \quad (3-10)$$

For a known \underline{a} the mass flow coefficient can thus be found. However, an equation is needed to relate C_H and \underline{a} in the brake state. If such a relation were known, it would be possible to properly optimize augmented systems. However, due to the lack of such a relationship, an estimate will be made for each system in turn.

3.4 DETERMINATION OF CAPACITY FACTOR

The capacity factor of a power producing device is a measure of the mean annual energy output compared to the maximum possible (the valid power). For wind energy systems, the Justus equation (Justus, et al, 1976) is used to find the capacity factor. This equation assumes that the wind speed distribution can be described by the Weibull equation:

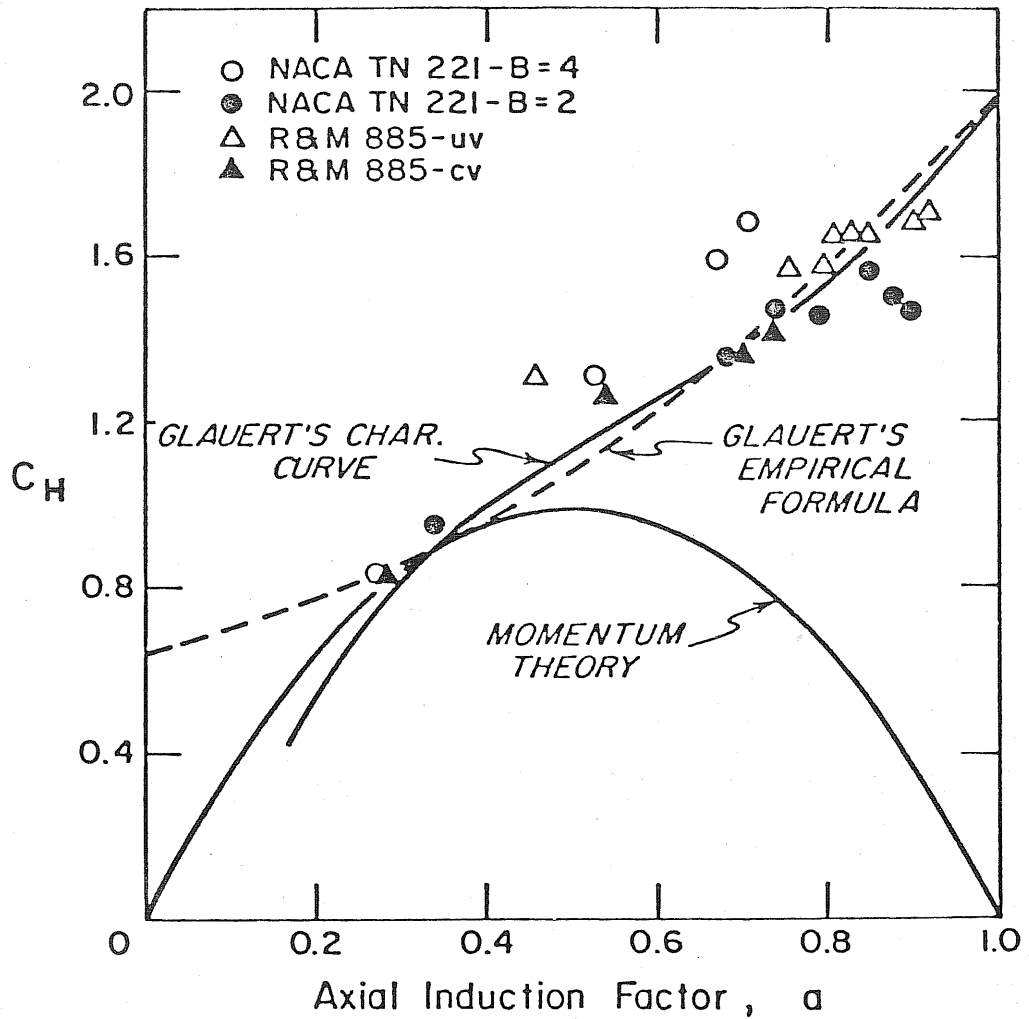


Figure 3-2. WINDMILL BRAKE STATE PERFORMANCE FOR AN UNAUGMENTED TURBINE (Source: Wilson, 1976)

$$p(V) = \exp\left(-\frac{V}{c}\right)^k, \quad (3-11)$$

where $p(V)$ is the fraction of the time the wind speed will be equal to or greater than V , and c is a scale parameter proportional to the average wind speed. The parameter, k , determines the shape of the distribution curve. The Weibull parameters were given by SERI for this report to be $c = 6.05$ m/s and $k = 2.27$.

In order to find the wind speed at the hub height of the turbine, it is necessary to assume a wind profile:

$$V_z = V_r \left(\frac{\ln(z/z_0)}{\ln(z_r/z_0)} \right), \quad (3-12)$$

where V_z is the wind speed at height z , V_r is the reference wind speed at the reference height z_r , and z_0 is a roughness parameter assumed equal to 0.05 meters. Again, the roughness length used was determined by SERI for this report.

The cut-in, rated, and cut-out wind speeds for all the configurations are taken to be 4.2, 7.5, and 18.2 meters per second, respectively, when measured at a height of 9.1 meters. These wind speeds are the Mod-X values, and to get a fair comparison, all other configurations are given the same values. This results in the same capacity factor for all systems. To understand this statement better, consider the following hypothetical situation.

All of the configurations are lined up side-by-side and subjected to the same wind field. When the wind speed, measured at 9.1 meters altitude, reaches 4.2 meters per second, all the systems cut-in. At 7.5 meters per second all the systems reach the rated power output of 200 kW, and they all cut-out at 18.2 meters per second. It is assumed that all the systems are designed to behave in this manner even though they all have different C_p 's and different hub heights. It follows immediately that at any given wind speed, the power output of all the systems is the same. Thus, for any given wind distribution over a period of time, the total number of kilowatt hours produced will be the same for all the systems, and hence the capacity factor is the same. Thus, the costs of the system become the effectiveness criteria since the output is identical.

For the values assumed above, the capacity factor is 0.39 for all the systems. This was obtained from the Justus equation.

3.5 SYSTEM EFFICIENCY

There are three main components that influence system efficiency: rotor efficiency, transmission efficiency, and the electrical system efficiency. For the Mod-X, the rotor power coefficient is 0.42, or 71% of ideal. The transmission efficiency is 94% and the generator efficiency is 94%, when at rated power output. This gives a power train efficiency of 89%, a system efficiency of 63%, and a system C_p of 0.37. It is assumed that these efficiencies are the same for all the systems under consideration, since for a proper comparison it is assumed that similar transmission and generator efficiencies are obtained.

3.6 PERFORMANCE OF THE AXISYMMETRIC STATIC INDUCER

AeroVironment has developed an analytical model for determining the augmentation of a ducted turbine. This model considers the duct to be a cylinder of vorticity of arbitrary strength. The distribution of this vorticity is found by matching the kinematic conditions to give the flow angle through the cylinder which corresponds to the local shape of the duct.

For example, for a simple 20-degree half angle divergent duct, a vorticity distribution is found which causes the flow angle near the cylinder wall to be at 20 degrees to the duct axis. The power extraction effects of the rotor are represented by a cylinder of vorticity that starts at the trailing edge of the duct and extends downstream to infinity. The perturbation of this semi-infinite cylinder on the flow through the cylinder representing the duct is then computed. This model is capable of finding the induction of ducts with divergence and camber. Inputs to the model are duct chord, divergence, and camber. Output is C_{M_O} and M_a . It should be noted that this model uses the radius of the duct camber line at the half chord point as the effective radius of the duct. The mass flow coefficients, and C_p are based on the duct area at this same point. This radius (or area) is called the hydrodynamic radius (or area) of the duct.

For the Grumman baseline diffuser, the chord is 0.87 of the hydrodynamic radius. The divergence angle is 30 degrees, giving an area ratio of 2.78. There is no camber. This gives a C_{M_O} of 1.82 and an M_a of 1.9. The optimum interference factor is 0.33, giving a C_p of 1.10. If C_p is based on turbine area we get $C_p = 1.96$, while, if based on exit area, we get $C_p = 0.71$. The AV duct theory is a linearized theory, and thus may not give a completely accurate estimate of the duct performance. Grumman has developed an exact vortex model for a conical ducted rotor. This model predicts a C_p of 2.13 for the baseline diffuser, based on turbine area which is comparable to the AV estimate. Wind tunnel tests made by Grumman have also achieved this performance level. The Grumman DUMP diffuser gets about 10% to 20% better performance than the baseline diffuser. This gives a C_p range of 2.16 to 2.56; a value of 2.37 was chosen for the AeroVironment high confidence predicted performance for the DUMP diffuser. This value is four times what can be achieved with a free turbine and is about the average of the expected range for the DUMP diffuser.

It is next necessary to consider operation in the brake state. In Figure 3-3 the experimental performance of the baseline diffuser is shown. The graph gives the dynamic pressure amplification (q at the turbine divided by q in the free stream) versus C_H . Shown are the Grumman data and the predicted performance according to AV theory. As can be seen, there is gross disagreement between the two curves. This may be due to viscous effects. The Grumman duct is equipped with slots for boundary layer control on the duct inner surface. These slots allow outside air to flow into the duct and re-energize the boundary layer. These slots perform better as the pressure in the duct is reduced due to the pressure drop across the turbine. Thus, at low C_H values, the duct may not have completely attached flow and will have lower performance than predicted. This explains the observed performance at C_H values of less than one. At C_H values greater than one, data indicates performance greater than predicted. This may be due to the scavenging effect mentioned previously.

Grumman has extrapolated this data and other test data high values of C_H , and found a maximum power point near a C_H of 2, giving a C_p of 3.74 for this configuration. This extrapolation may not be valid as there is no data near this C_H value to indicate if the curve remains linear. Grumman feels that a scaled-up version using the DUMP diffuser

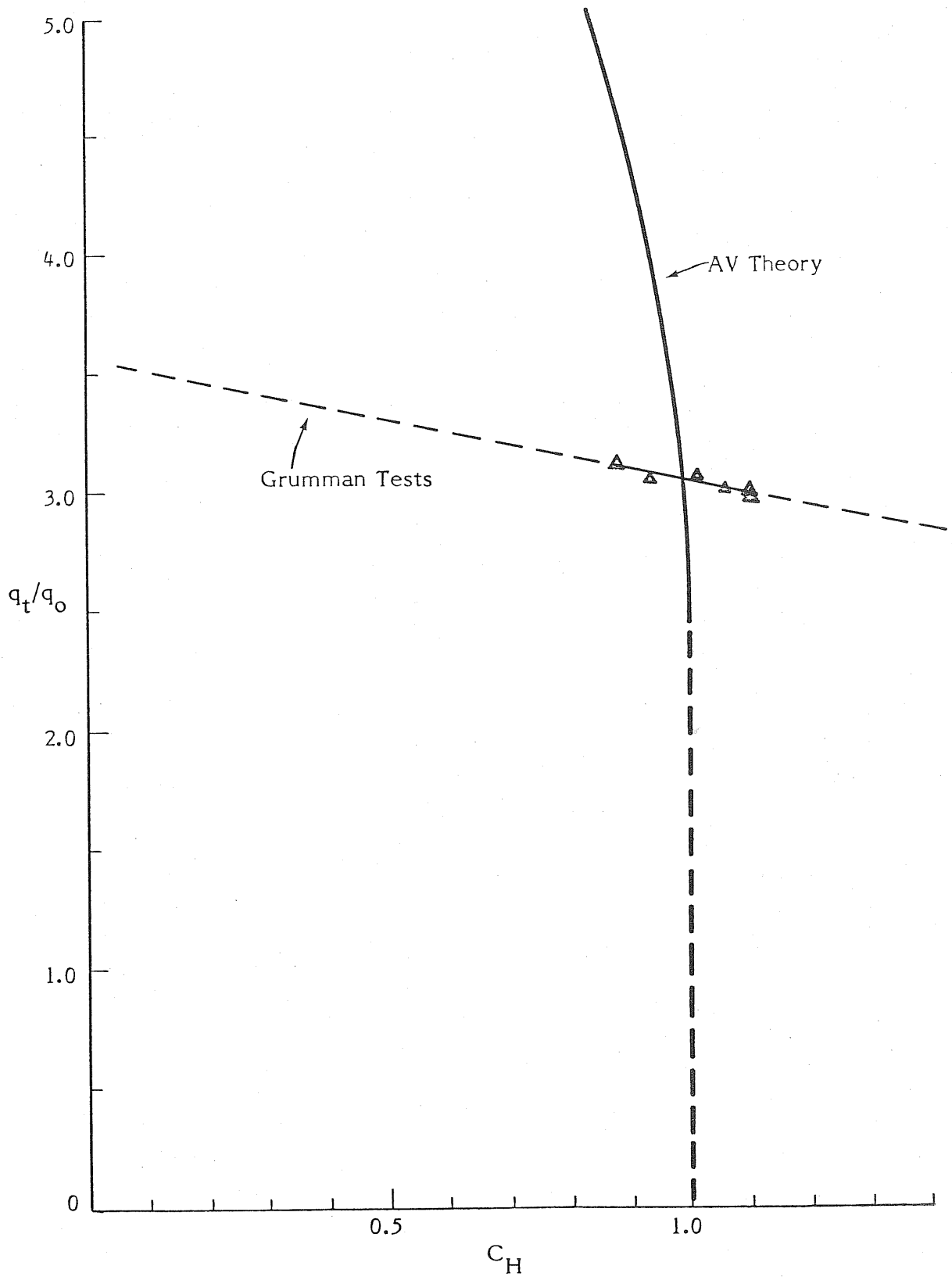


Figure 3-3. PRESSURE AMPLIFICATION VS HEAD LOSS FOR THE GRUMMAN DUCT

will have a C_p of 4.74 (eight times that of a free turbine, Foreman, 1979). This is the value used for the Grumman extrapolated performance of the diffuser.

3.7 PERFORMANCE OF THE PLANAR STATIC INDUCER

The planar static inducer under consideration consists of a delta wing with a 75-degree leading edge sweep back. The delta is assumed to be at an angle of attack of 29 degrees. The turbines placed above the delta in each of the leading edge vortices has a diameter equal to 0.33 times the span of the delta.

The axial velocity above one-half of the delta is shown in a contour plot in Figure 3-4. The circle swept out by the turbine is also shown. The average mass flow coefficient for this circle is 1.82. The turbine is essentially a free turbine, hence M_0 is equal to one. This gives a C_p of 1.38, based on turbine area. Based on delta wing planform area, the C_p is 0.25. This is the AeroVironment high confidence estimate for the planar static augmentor.

It is next necessary to consider if any performance increase can be obtained by operating in the brake state. The higher power output of this device can only be realized if such operation is possible. When operating in the brake state, the air that has gone through the turbine has insufficient energy to overcome the adverse pressure gradient at the trailing edge of the delta wing. If this flow is properly scavenged, high power output may be possible. However, if this flow develops a reverse flow region, the result may be flow separation from the delta and loss of augmentation. Figure 3-5 shows these two situations. As can be seen in the unsuccessful scavenging case, a reversed flow region could effectively block flow through the turbine.

Sforza has assumed that the turbine will produce power as though it were a free turbine operating in an increased velocity flow field. This leads to the conclusion that the optimum C_H is increased by the square of C_{M_0} over the optimum for a normal windmill ($= .89$), and C_p increases by the cube of C_{M_0} . For the configuration under study, this would result in a C_p of 3.63 and a C_H of 2.98. It is felt that these values are too large to be achievable in practice. A C_H of 2.0 was selected as a maximum possible value. This value is the same as the maximum possible for a free turbine and is the value assumed for the duct when operating in the brake state. This gives a C_p of 2.99. This is the assumed extrapolated performance case for the planar static augmentor.

3.8 PERFORMANCE OF THE DYNAMIC INDUCER

van Holten (1978) has recently completed experimental investigations into the dynamic inducer that indicate that a C_{M_0} of 3.0 is achievable. His inducer model consisted of two blades with a span and chord (normalized by the model radius) of 0.63 and 0.40, respectively. The inducer blades operated at a C_L of 0.67. The model was run at an advance ratio of 10. The blade span is twice what was assumed for the previous dynamic inducer report done by AeroVironment. Previously, it was assumed that the blade span had to be chosen so that the blade would operate in the "vortex synchronous state," where the vortex from the upwind tip of one inducer blade is cancelled out by the downwind tip of the next inducer blade. This results in a situation with no shed vorticity, and hence no induced drag. In this study the inducer blades will be given a normalized span of 0.32, preserving the vortex synchronous state. This will give a C_{M_0} of 2.0, one-half the increase caused by the longer inducer blades over the unaugmented case.

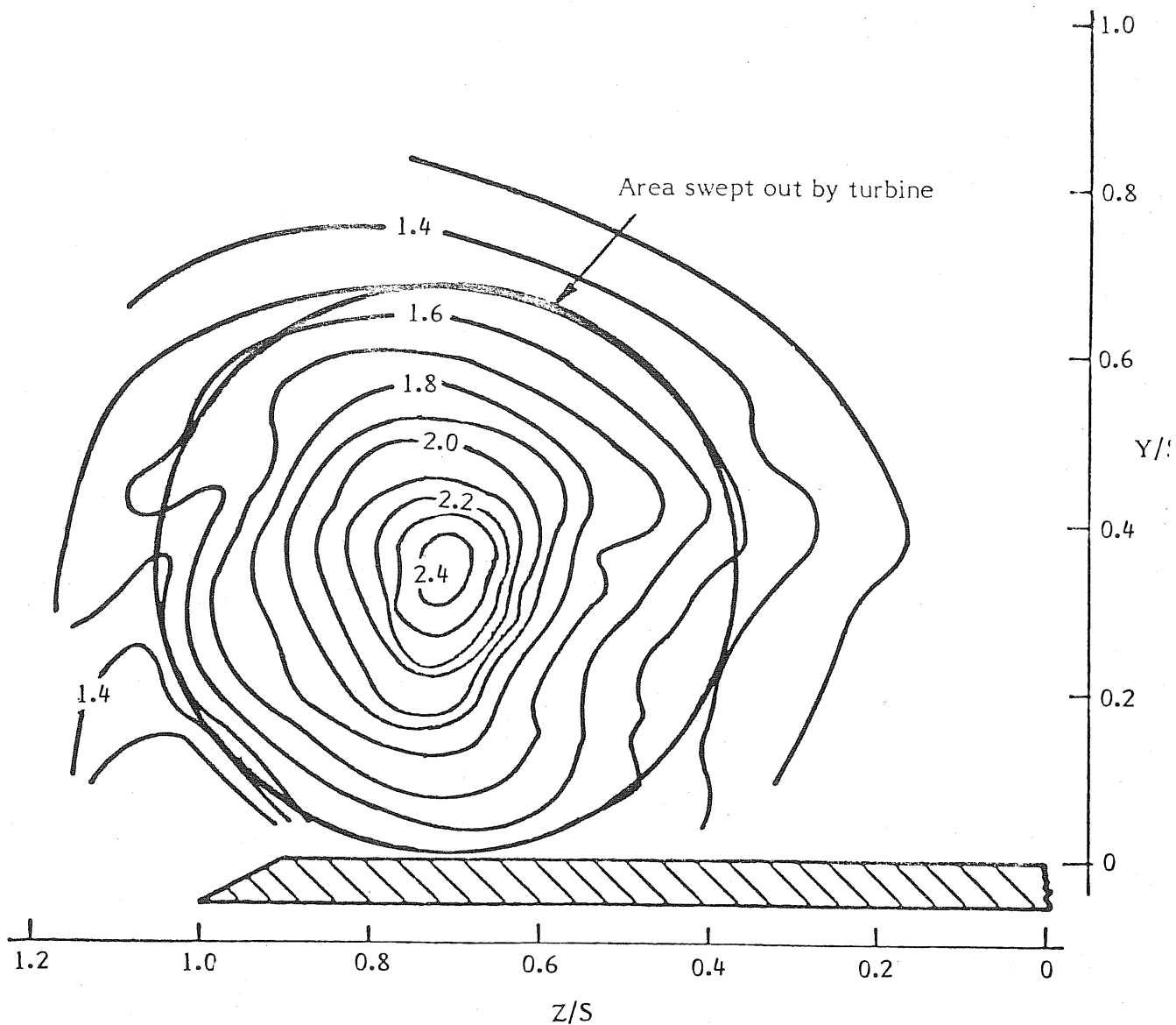


Figure 3-4. CONTOURS OF CONSTANT VELOCITY MAGNITUDE FOR VORTEX FIELD ABOVE BASIC VORTEX AUGMENTOR SURFACE AT AN ANGLE OF ATTACK OF 29 DEGREES

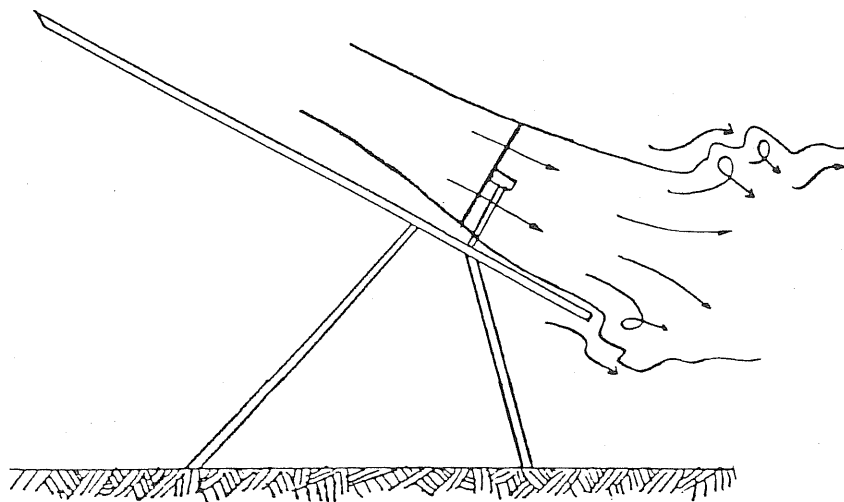


Figure 3-5a. VORTEX AUGMENTOR IN THE WINDMILL BRAKE STATE WITH SUCCESSFUL SCAVENGING

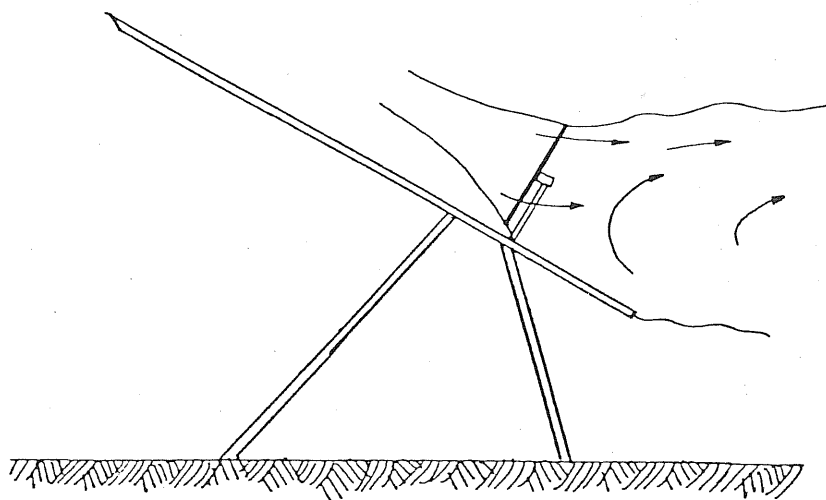


Figure 3-5b. VORTEX AUGMENTOR WITH UNSUCCESSFUL SCAVENGING

The value of M for the dynamic inducer turbine is that of a free turbine, namely, 1. This gives a C_P of 1.56. The inducer blades cause a power loss due to their viscous drag. The blades in van Holten's tests were operating at a low Reynolds number and could not generate a high C_L . For this analysis it is assumed that a high lift, low drag airfoil can be used, giving a C_L of 1.5 with a C_D of 0.01. This reduces the required non-dimensional blade chord to 0.2, keeping CC_L equal to 0.3. The power coefficient due to viscous loss is:

$$C_{P_L} = \frac{X^3 N C_b C_D}{\pi} \quad (3-13)$$

For this particular case, this results in a C_{P_L} of 0.4, giving a total C_P of 1.16. This is the high confidence estimate.

It is now necessary to consider operating in the brake state. Figure 3-5 shows the relationship between \underline{a} and C_H for a free propeller, the closest case to a dynamic inducer for which there is data. This data indicates that the relationship between \underline{a} and C_H can be approximated by

$$C_H = 2a \quad (3-14)$$

for high values of \underline{a} . Using this relation, it is possible to optimize the C_P equation and get

$$C_{P_{\max}} = \frac{C_{M_O}^2}{2M_a} \quad (3-15)$$

when

$$a = \frac{C_{M_O}}{2M_a} \quad (3-16)$$

For the case under consideration, this gives a C_P of 2.0 when \underline{a} is 1.0. This corresponds with a value of 2.0 for C_H , which is the same C_H^{\max} assumed for the previous extrapolated configurations. The power loss due to the inducer blades will be the same as before (0.4), giving a total C_P of 1.60. This is the extrapolated performance estimate for the dynamic inducer.

3.9 ACTUAL SYSTEM PERFORMANCE

Up to now C_P 's have been computed assuming a perfect turbine and power train. However, the turbine efficiency is assumed to be 71% and the power train efficiency is 88.5%. This allows the computation of a rotor C_P and a system C_P . These values are shown in Table 3-1. Also shown is the ideal C_P of each system divided by 0.593, the Betz limit. This is the ideal augmentation ratio. Note that in the case of the dynamic inducer, the rotor C_P is multiplied by the rotor efficiency before the power loss due to the inducer blades is considered. The inviscid value is C_{P_i} , which is the C_P with no losses of any kind.

Table 3-1. CONFIGURATION POWER COEFFICIENTS

Configuration	C_P Ideal	C_P Rotor	C_P System	Ideal Augmentation Ratio
Axisymmetric, static, high confidence	2.37	1.68	1.47	4.00
Axisymmetric, static, extrapolated	4.74	3.36	2.95	8.00
Planar, static, high confidence	1.36	0.96	0.85	2.29
Planar, static, extrapolated	2.99	2.12	1.86	5.04
Dynamic, high confidence	1.56	0.71	0.63	2.63
Dynamic, extrapolated	2.00	1.02	0.90	3.37
Mod-X	0.59	0.42	0.37	1.00

3.10 ROTOR SIZES

If all the configurations had the same hub height or the vertical wind profile was constant, then the rotor sizes would scale directly. However, each configuration has a different hub height corresponding to different rotor diameter. For each system, a ratio between hub height and rotor radius was assumed. Then for each configuration a size was found which would give that configuration the same power output as the Mod-X when both are in the same wind field. The hub height to rotor radius ratios chosen are equal to those of the current designs of the investigators of the various systems, and are as follows:

System	Hub Height/Rotor Radius
Mod-X	1.6
Axisymmetric static inducer	2.2
Planar static inducer	5
Dynamic inducer	1.67

For the Mod-X, this corresponds to a rotor radius of 62.5 feet and a hub height of 100 feet. Grumman's current design proposal for the axisymmetric static inducer calls for an 18-foot rotor diameter mounted at a hub height of 20 feet. This is the proposed configuration for testing at Rocky Flats. The hub height to rotor radius ratio for the planar static inducer comes from the dimensions of Sforza's field test model currently under study. For the dynamic inducer, the hub height is assumed to be 1.6 times the radius of the rotor plus tip-vane assembly, where the tip-vanes are coned at 17° to horizontal.

For the planar static inducer, Sforza has claimed that the delta wing brings down air from a still higher level to the rotors. This does not seem to be the case, since the air that flows over the top of a lifting wing originates from below that wing, and the influence of a lifting wing is normally to induce an upward component on the airflow upstream of the unit.

Table 3-2 gives the resulting rotor radius for each configuration, as well as the hub height, and rotor area ratioed to that of the Mod-X. Also shown is the ratio between the C_p for each system (including all losses) ratioed to the C_p of the Mod-X (0.37). This is the system augmentation ratio.

Figures 3-6a and 3-6b are sketches which show the relative sizes of each unit for the high confidence and extrapolated cases.

Table 3-2. CONFIGURATION ROTOR SIZES

Configuration	Rotor Radius (Meters)	Hub Height (Meters)	Area Ratio	System Augmentation Ratio
Axisymmetric static, high confidence	10.73	23.61	3.15	4.00
Axisymmetric static, extrapolated	8.50	18.70	5.02	8.00
Planar static, high confidence	7.98	39.91	2.85	2.29
Planar static, extrapolated	6.05	30.23	4.96	5.04
Dynamic, high confidence	16.40	27.39	1.35	1.70
Dynamic, extrapolated	14.47	23.16	1.74	2.43
Mod-X	19.06	30.48	1.00	2.43

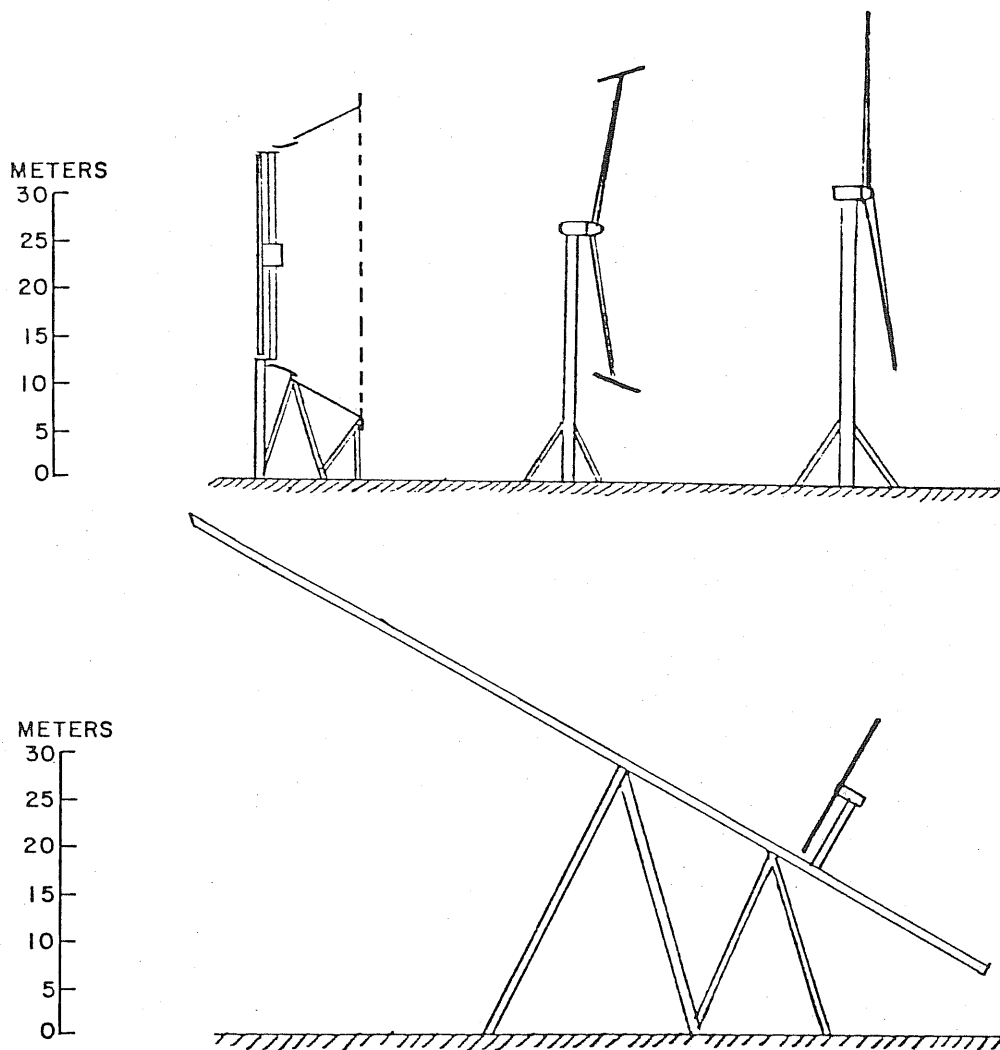


Figure 3-6a. SKETCHES OF WIND TURBINES DESIGNED FOR THE HIGH CONFIDENCE LEVEL DESIGN

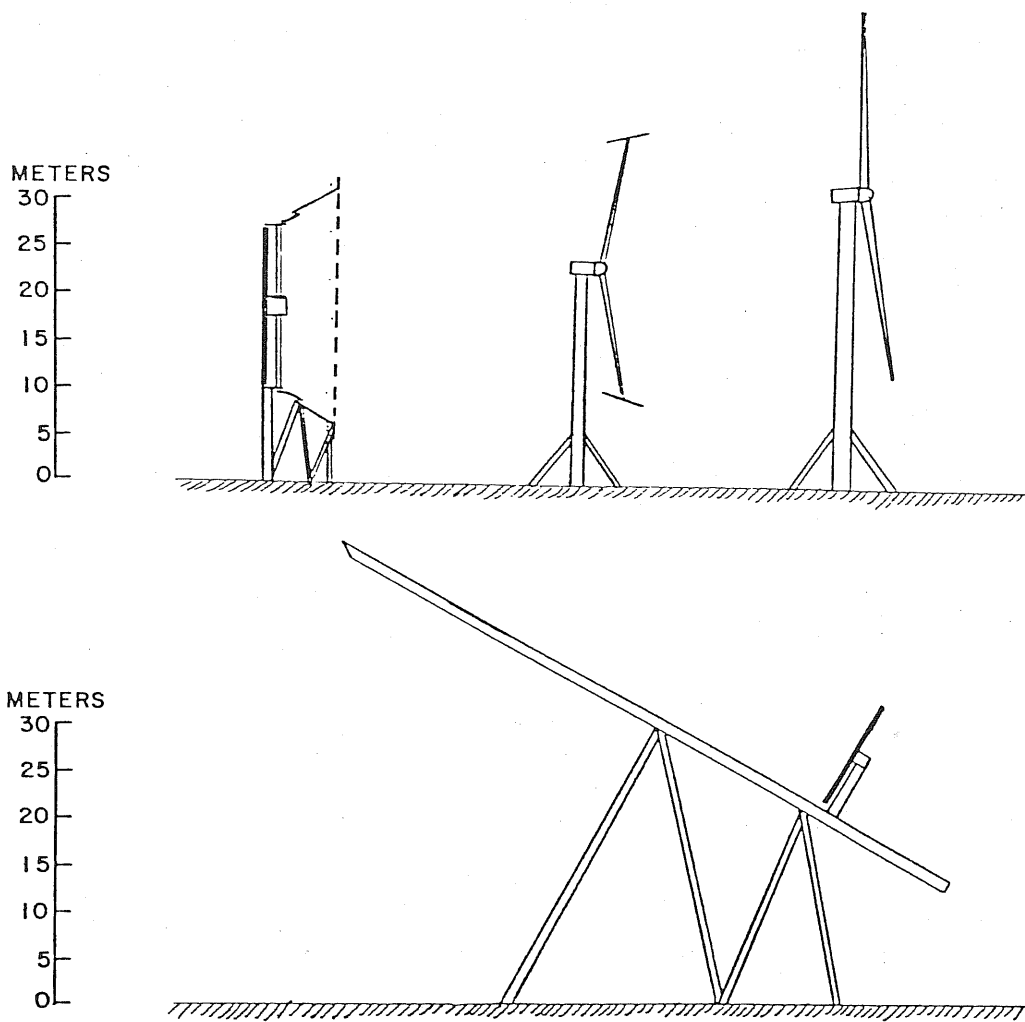


Figure 3-6b. SKETCHES OF WIND TURBINES DESIGNED FOR THE EXTRAPOLATED LEVEL DESIGN

SECTION 4.0

COST ANALYSIS

4.1 COST OF COMPONENTS

In order to find the cost of each of the configurations under consideration, each was divided up into a number of components. The cost of each component is then scaled in an appropriate way to the cost of the similar component in the Mod-X. The cost and weight of each component is discussed below. All costs are for the hundredth unit and estimated in 1978 dollars.

4.1.1 Rotor

The Mod-X rotor has a radius of 19.1 meters and a solidity of 3% (NASA 1979). This gives a blade area of 34.2 square meters. The rotor cost is \$30,000 and its weight is 2,132 kg. The rotor cost is thus \$877 per square meter and it weighs 62.34 kg per square meter. The rotor solidity, weight per unit area and cost per unit area are assumed to be the same regardless of rotor radius for all the configurations under consideration.

The assumption on solidity can be made because it has been shown that the most efficient rotor design has the same planform, regardless of rotor size, and thus gives the same solidity (Wilson, 1976). The weight and cost assumption is based on General Electric's work on the weight and cost of wind turbine rotors (G.E., 1976). Although the absolute values given in that work may be dated, it is believed here that the trend in weights and costs with rotor size changes is correct. This appears to be a conservative assumption, since the Mod-X has the largest diameter of all rotors considered, and since it is expected that the rotor cost per unit area will increase somewhat for larger radius rotors.

4.1.2 Hub/Pitch Control

The hub and blade pitch control mechanisms are all considered as one unit. For the Mod-X this unit costs \$16,820 and weighs 2,041 kg. The weight and cost of this component are assumed to be proportional to the rotor weight. This gives a hub cost of \$7.89 per kg of blade weight, and a hub weight of 0.957 times the blade weight.

4.1.3 Bedplate and Gearbox

The Mod-X design considers the bedplate and gearbox as a integrated unit. This helps lower costs, as this unit must absorb the torque loads generated by the rotor. The primary cost driver for the gearbox is not the gear ratio, but the power level that the gearbox must handle. This can be seen from G.E.'s work (G.E., 1976). So even though the gear ratio is different for different configurations, this component is assumed to have the same weight and cost for all the configurations under consideration. For the Mod-X the bedplate/gearbox is 7,484 kg and the cost is \$26,400.

4.1.4 Electrical System

This component includes generator, power conditioning, transformers, circuit breakers, and controls. It is assumed to have the same weight and cost for all the configurations under consideration. The weight is 2,495 kg and the cost is \$11,700.

4.1.5 Tower

The tower on the Mod-X rotates for yaw control. The cost of the tower includes the yaw mechanism which is passive. The tower cost is given by the following equation:

$$C = 26072 + 5.26 \cdot 10^{-3} T_E h_t \text{ (dollars) ,} \quad (4-1)$$

where T_E is the equivalent downwind thrust in Newtons, including a 2.3 load factor for intermittent and dynamic loading, and h_t is the tower height in meters. This equation came from the General Electric study^t(1976) after a simple modification. The GE equation was for a truss-type tower that did not rotate. The Mod-X rotating tower is a simple round cylinder. To get the equation to give the correct cost for the Mod-X, the equation was multiplied by a constant factor of 1.38.

The thrust, T_E , can be found from:

$$T_E = 4.4076 C_{M_O} C_H R^2 V^2 \text{ Newtons ,} \quad (4-2)$$

where V is the rated velocity at hub height. The cost of the Mod-X tower is \$45,190 and it weighs 18,824 kg or \$2.40 per kg. Other towers have the same weight-to-cost ratio. The static inducer systems are assumed to have the tower structure integrated with the augmentor surface. The cost of the tower/augmentor structure is considered as a single component, described below, so a separate tower cost is not considered for these configurations. Thus, the above equation is only used for the dynamic inducer system.

4.1.6 Augmentor

For the dynamic inducer, the cost of the induction blades is equal to the cost of the rotor blades on a per area basis. The inducer blade weight scales similarly. The inducer blade weight is included in the total rotor weight for computing the hub costs.

Cost data from Grumman was used in evaluating the static inducers. This data indicates that for a 2.74-meter radius inlet, a prototype DUMP diffuser-type duct would cost \$44,000. Assuming a 90% learning curve, this gives a \$22,000 cost for the hundredth unit. The surface area of this duct is approximately 70 square meters, and the duct weight is 3,000 kg. (The exact design of this duct is currently Grumman proprietary.) This gives a cost per square meter of \$314 and a weight of 42.86 kg per square meter. These costs and weights per square meter are assumed to be constant for all the static inducer configurations, both axisymmetric and planar.

The static inducer component is assumed to include the inducer surface, the tower, the yaw mechanism, and the nacelle support. Thus, a separate tower cost is not included in the cost analysis.

4.1.7 Foundation

The foundation supports the entire structure. Its cost for the Mod-X is \$4,000. For other systems, the cost of the foundation scales to the weight it must support. The weight of the entire Mod-X is 32,972 kg, giving a foundation cost of \$0.1213 per kg of supported structure.

4.1.8 Other Costs

After all of the above costs are added up, a 14.35% miscellaneous charge is added on. This charge includes controls, safety equipment, testing, shipping and installation. On top of this is placed a 15% charge for G&A, and on top of that is placed a 15% profit. This results in a 51.23% increase over the basic component costs.

Maintenance cost estimates for the Mod-X place this cost at \$4,000 per year. Over a 30-year lifetime, including inflation, the maintenance costs are expected to rise, resulting in a 30-year levelized cost of \$7,500 per annum in 1978 dollars.

4.2 SYSTEM POWER COSTS

Using the above information the total costs of each configuration can now be found. The cost of electricity for each configuration is found from:

$$\text{cost per kWh} = \frac{\text{Total cost} \times \text{annual charge factor} + \text{yearly maintenance}}{\text{Total kWh produced per year}}, \quad (4-3)$$

where the annual charge factor is 18%, maintenance is taken at the 30-year average of \$7,500/yr, and 697,949 kWh are produced per year. It is noted that since the annual charge rate and delivered power are the same for all configurations, the maintenance cost of about 1.07 ¢/kWh is the same for all.

4.2.1 Mod-X

Table 4-1 shows the cost breakdown for the Mod-X. The total installed system cost is \$202,805 or \$1,015 per kW. The cost of electricity is 6.3 cents per kWh.

4.2.2 Axisymmetric Static Augmentor

The surface area of the duct can be found from:

$$\text{duct area} = 9.324R^2 \quad (4-4)$$

Table 4-1. MOD-X COST BREAKDOWN

Component	Weight (kg)	Cost (\$)
Augmentor	0	0
Blades	2,132	30,000
Hub and Pitch Control	2,041	16,820
Bedplate and Gearbox	7,480	26,400
Electrical System	2,495	11,700
Tower	18,824	45,190
Foundation	-	4,000
Subtotal	32,972	134,110
Miscellaneous at 14.35%		19,245
Subtotal		153,355
G&A at 15%		23,000
Subtotal		176,355
Profit at 15%		26,450
TOTAL		<u>\$202,805</u>
O & M		\$ 7,500

Annual kWh: 697,950
 Cost per kW installed: \$ 1,015
 Cost per kWh: 6.3¢

This gives a duct area of $1,073.5 \text{ m}^2$ for the high confidence case and 673.7 m^2 for the extrapolated case. Using the costing methods outlined above, we find that the high confidence configuration total cost is \$600,450 or \$3,00 per kW installed. The cost of electricity is 16.6 cents per kWh.

For the extrapolated configuration the total cost is \$398,965, or \$1,995 per kW installed. The cost of electricity for this configuration is 11.4 cents per kWh. Tables 4-2 and 4-3 give the details of the cost breakdown. As can be seen in these tables, the major cost item is the duct itself. This one component costs more than the entire Mod-X.

4.2.3 Planar Static Inducer

The area of the augmentor surface can be found from:

$$\text{augmentor area} = 36R^2 \quad (4-5)$$

This gives an area of $2,292 \text{ m}^2$ for the high confidence case and $1,318 \text{ m}^2$ for the extrapolated case. In doing the cost analysis, it must be remembered that this system has two rotors; however, the total bedplate/gearbox and electrical costs are assumed the same, although these components may be divided into two smaller units.

The cost for the high confidence configuration is \$1,191,040, or \$5,955 per kW. The cost of electricity is 31.8 cents per kWh. Table 4-4 gives the cost breakdown. For the extrapolated configuration, the total cost is \$710,150 or \$3,550 per kW installed; the cost of electricity is 19.4 cents per kWh. Table 4-5 gives the cost breakdown for this configuration. As can be seen in the cost breakdown, the augmentor surface utterly dominates the cost of the configuration. This is due to the intensity of this surface. For the high confidence case, the delta wing is 96 meters long and 48 meters wide, a size comparable to a football field. Even the extrapolated case has a length of 72 meters and a width of 36 meters.

4.2.4 Dynamic Inducer

The area of the inducer blades can be found from:

$$\text{inducer area} = 0.126R^2 \quad (4-6)$$

This gives an area of 33.8 m^2 for the high confidence case and 26.4 m^2 for the extrapolated case. As can be seen, the area of these inducer surfaces is much lower than the area of the static inducers; however, the cost per unit area is greater.

To find the tower costs it is necessary to first find the downwind load on the tower. For the high confidence case this is 168,113 Newtons, and for the extrapolated case, 269,621 Newtons. (For the Mod-X the downwind load is 119,482 Newtons.)

The total cost of the high confidence system is \$262,750, or \$1,314 per kW. The cost of electricity for this configuration is 7.8 cents per kWh. For the extrapolated case the cost is \$249,925 or \$1,250 per kW installed. The cost of electricity is 7.5 cents per kWh. The cost breakdowns are shown in Tables 4-6 and 4-7.

Table 4-2. COST BREAKDOWN FOR AXISYMMETRIC STATIC INDUCER, HIGH CONFIDENCE

Component	Weight (kg)	Cost (\$)
Augmentor	46,010	337,079 (84%)
Blades	677	9,524
Hub and Pitch Control	648	5,396
Bedplate and Gearbox	7,480	26,400
Electrical system	2,495	11,700
Tower	0	0
Foundation	-	6,952
Subtotal	57,310	397,051 (100%)
Miscellaneous at 14.35%		56,977
Subtotal		454,028
G&A at 15%		68,102
Subtotal		522,13
Profit at 15%		78,320
TOTAL		<u>\$600,450</u>
O & M		\$ 7,500

Annual kWh: 697,950
 Cost per kW installed: \$ 3,000
 Cost per kWh: 16.7¢

Table 4-3. COST BREAKDOWN FOR AXISYMMETRIC STATIC INDUCER, EXTRAPOLATED

Component	Weight (kg)	Cost (\$)
Augmentor	28,874	211,542 (80%)
Blades	425	5,976
Hub and Pitch Control	407	3,387
Bedplate and Gearbox	7,480	26,400
Electrical System	2,495	11,700
Tower	0	0
Foundation	-	4,813
Subtotal	39,681	263,818
Miscellaneous at 14.35%		37,858
Subtotal		301,676
G&A at 15%		45,251
Subtotal		346,927
Profit at 15%		52,038
TOTAL		<u>\$398,965</u>
O & M		\$ 7,500

Annual kWh: 697,950
 Cost per kW installed: \$ 1,995
 Cost per kWh: 11.4¢

Table 4-4. COST BREAKDOWN FOR PLANAR STATIC INDUCER, HIGH CONFIDENCE

Component	Weight (kg)	Cost (\$)
Augmentor	98,235	719,688 (91%)
Blades	748	10,526
Hub and Pitch Control	716	5,962
Bedplate and Gearbox	7,480	26,400
Electrical System	2,495	11,700
Tower	0	0
Foundation	-	13,303
Subtotal	109,674	787,579
Miscellaneous at 14.35%		113,018
Subtotal		900,597
G&A at 15%		135,090
Subtotal		103,567
Profit at 15%		155,353
TOTAL		<u>\$1,191,040</u>
O & M		\$ 7,500

Annual kWh: 697,950
 Cost per kW installed: \$ 5,955
 Cost per kWh: 31.8¢

Table 4-5. COST BREAKDOWN FOR PLANAR STATIC INDUCER, EXTRAPOLATED

Component	Weight (kg)	Cost (\$)
Augmentor	56,489	413,852 (88%)
Blades	430	6,048
Hub and Pitch Control	412	3,427
Bedplate and Gearbox	7,480	26,400
Electrical System	2,495	11,700
Tower	0	0
Foundation	-	8,164
Subtotal	67,306	469,591
Miscellaneous at 14.35%		67,386
Subtotal		536,977
G&A at 15%		80,547
Subtotal		617,524
Profit at 15%		92,626
TOTAL		<u>\$710,150</u>
O & M		\$ 7,500

Annual kWh: 697,950
 Cost per kW installed: \$ 3,550
 Cost per kWh: 19.4¢

Table 4-6. COST BREAKDOWN FOR DYNAMIC INDUCER, HIGH CONFIDENCE

Component	Weight (kg)	Cost (\$)
Augmentor	2,110	29,686 (17%)
Blades	1,577	22,188
Hub and Pitch Control	3,528	29,385
Bedplate and Gearbox	7,480	26,400
Electrical System	2,495	11,700
Tower	20,744	49,786
Foundation	-	4,601
Subtotal	37,934	173,746
Miscellaneous at 14.35%		24,933
Subtotal		198,679
G&A at 15%		29,802
Subtotal		228,481
Profit at 15%		34,269
TOTAL		<u>\$262,750</u>
O & M		\$ 7,500

Annual kWh: 697,950
 Cost per kW installed: \$ 1,314
 Cost per kWh: 7.8¢

Table 4-7. COST BREAKDOWN FOR DYNAMIC INDUCER, EXTRAPOLATED

Component	Weight (kg)	Cost (\$)
Augmentor	1,645	23,135 (19%)
Blades	1,228	17,282
Hub and Pitch Control	2,749	22,898
Bedplate and Gearbox	7,480	26,400
Electrical System	2,995	11,700
Tower	24,549	58,918
Foundation	-	4,930
Subtotal	40,646	165,263
Miscellaneous at 14.35%		23,715
Subtotal		188,978
G&A at 15%		28,347
Subtotal		217,325
Profit at 15%		32,600
TOTAL		<u>\$249,925</u>
O & M		\$ 7,500

Annual kWh: 697,950
 Cost per kW installed: \$ 1,250
 Cost per kWh: 7.5¢

4.3 DISCUSSION

Table 4-8 shows the costs of all configurations under consideration, the cost ratio to the Mod-X, the cost of electricity from each, and the cost of electricity ratioed to that of the Mod-X. As can be seen, none of the augmented systems were found to be more cost-effective than the Mod-X. The most cost-effective augmented system is the dynamic inducer, followed by the ducted turbine and, last, by is the vortex augmentor. The failure of all the augmented systems to show cost-effectiveness requires some examination. All the augmented systems have power coefficients that are at least twice as large as that of the Mod-X, so at first glance one would expect that the augmented systems would be more cost-effective. In fact, all the augmented systems succeed in their preliminary intention, the decrease of rotor costs. At first glance, it would seem that if the rotor costs are lower, then the cost of electricity generated by the system will be lower, which is the primary reason for the augmentation systems. The assumption that lower rotor costs mean lower electricity costs is based upon the assumption that the rotor is a very large cost item. However, the Mod-X rotor is only 22% of the total component cost. Thus, reducing rotor costs can only result in a more cost-effective system if the augmentor is also extremely low cost. None of the augmentors under consideration meet this requirement.

To further illustrate this idea, Table 4-9 shows the power coefficient of each configuration when the reference area is the total aerodynamic surface area (augmentor + rotor) of that configuration. Static augmentation surfaces are shown to have only 1.4% to 9% the C_p of the Mod-X. The cost of static augmentors is about 36% that of rotor blades on a per-area basis, so it is easy to see why they are not cost-effective. The dynamic inducer has a much higher C_p based on aerodynamic surface area, and is comparable to the C_p of the Mod-X. Unfortunately, high downwind loads made the tower more costly, even though it was shorter. The shorter tower places the rotor in a lower wind area, and hence requires a larger rotor. However, in general, systems with a higher C_p based on aerodynamic surface area will tend to be more cost-effective.

At this level of analysis, the interaction of higher stresses and loads with improved C_p and rotor costs has not been considered. However, it is expected that any error thus caused will be small because the rotor costs are small in comparison to the total system cost for the augmented systems.

Table 4-8. SUMMARY OF CONFIGURATION COSTS

Configuration	Total Cost (Dollars)	Total Cost Ratioed to Mod-X	Cost of Electricity (¢ per kWh)	Cost of Electricity Ratioed to Mod-X
Mod-X	202,805	1.0	6.3	1.0
Axisymmetric static high confidence	600,450	3.0	16.6	2.6
Axisymmetric static, extrapolated	398,965	2.0	11.4	1.8
Planar static, high confidence	1,191,040	5.9	31.8	5.0
Planar static, extrapolated	710,150	3.5	19.4	3.0
Dynamic, high confidence	262,750	1.3	7.8	1.2
Dynamic, extrapolated	249,925	1.3	7.5	1.2

Table 4-9. C_p BASED ON AERODYNAMIC SURFACE AREA

Configuration	Aerodynamic Surface Area Divided by Rotor Area	C_p Based on Rotor Area	C_p Based on Aerodynamic Surface Area
Mod-X	0.03	0.42	14.03
Axisymmetric static high confidence	3.00	1.08	0.56
Axisymmetric static extrapolated	3.00	3.37	1.12
Planar static, high confidence	5.76	0.97	0.17
Planar static, extrapolated	5.76	2.12	0.37
Dynamic, high confidence	0.07	0.71	10.09
Dynamic, extrapolated	0.07	1.02	14.53

SECTION 5.0

OUTLINE OF PROGRAM PLAN FOR FURTHER DEVELOPMENT OF AUGMENTOR SYSTEMS

5.1 SUMMARY OF AUGMENTOR PRINCIPLES

It is convenient to discuss here the basic augmentor principle as a foundation for the recommendations for further work. First, we note that all augmentors operate by inducing a larger mass flux through the actuator disk than would occur in the free actuator case. This can be accomplished only by increasing the axial velocity through the actuator, and no additional effect is achieved by inducing rotational components. There is no way of increasing the total head per unit mass of the free stream flow except by doing work on it, and in an ideal system this work would be the same amount as the additional energy available. In a real system, with losses, the additional available energy would be less than the work done on the flow. However, it is clearly possible to accelerate the axial flow, thus, in effect, drawing air from a greater cross-sectional area than that associated with the actuator or power extraction disk.

It is helpful here to consider the no-load amplification; that is, the ratio of the mass flow through the actuator at no load compared with the mass flow through a free actuator with no augmentation. This provides an upper bound (at least in the inviscid case) on the maximum flux of air from which energy can be extracted, since the far downstream wake velocity theoretically should not be lower than about one-third free stream. Thus, the energy extraction can be computed from the mass flux and the wake head loss. Consequently, the augmentation potential should be based on the speed through the disk or the mass flux, and not on the cube of this speed. Next, we note that as power is drawn from the actuator disk the resistance of the system will increase, so that the amplification will drop below that for the no-load case. The determination of the flux amplification with power production is a nontrivial problem, which is different for various types of augmentors, and has been treated by both analytical and experimental techniques.

Next, we note that if the far wake is assumed to have a velocity of $V(1 - 2a)$, where V is the free wind speed, then the drag on the entire system, D_S , is given by $D_S = 2 M Va$, where M is the mass flow through the system. However, the ideal power extracted is given by $P_i = M \Delta p$, where Δp is the wake head loss. This can be rewritten

$$P = D_S V(1 - a) , \quad (5-1)$$

if all the flow affected by the inducer passes through the actuator. This illustrates the point that, ideally, the tower drag which will be equal to D_S is independent of the inducer system for the inviscid flow in this case. However, a real inducer produces drag under the no-load case, which occurs due to viscous drag effects in the dynamic inducer and the duct, and due to both viscosity and lift-induced drag in the case of the planar static inducer. Thus, a price of increased tower load must be paid for all inducer systems as compared with a free wind turbine.

We note also that for all inducer systems the efficiency of the rotor system itself becomes very significant because the viscous losses are related to the local flow speed and are thus accentuated by induction. So, augmented systems will benefit more by increased rotor efficiency, just as a high-speed aircraft benefits more by viscous drag reduction.

Finally, we note that, in the most general terms, the effectiveness of augmentors must be related to the amount of amplification per unit area of augmentor device, and to the basic trade-off of this cost versus the cost of a larger free turbine, taking into account any structural benefits gained by using the augmentor. In this respect, it appears that the axisymmetric static inducer (duct) and the dynamic inducer appear to be the optimal way of speeding up the largest amount of air most effectively, and are coupled properly to the circular power extraction surface of the propeller-type turbine. Although the duct and the dynamic inducer represent the static and the dynamic augmentation principle, their aerodynamic effects are essentially the same -- creating an accelerated circular stream tube at the actuator. There is a direct analogy with the helicopter and the fixed-wing aircraft; both create the vertical acceleration within the span of the device, with the dynamic system (the helicopter) achieving an advantage of reduced lifting surface area at the price of power required to drive this surface. The planar static inducer appears configurationally inefficient here, since portions of the accelerated air do not pass through the power extraction device. In this case, one concludes that the entire area of the augmentor is not being used efficiently, since only part of it is required to develop the required induced flow stream from which power is extracted. Moreover, an additional no-load tower drag is present, due to the induced drag of the planar lifting system.

Thus, the criteria by which an augmentor may be judged are the no-load mass flux amplification, the effects of power extraction on this amplification (that is, how much the amplification is reduced), the total system dragwise load created by the augmentor and power extraction system, and the surface area (or, more significantly, the cost) of the required augmentor.

A further important fluid-mechanical issue arising here is the possibility that the augmentor makes it possible for the external flow to assist in scavenging the actuator flow. The idea here is as follows: in an ideal inviscid system one can compute the actuator load for maximum power extraction. The limits are imposed by the condition that as head is extracted from the flow the mass flux through the actuator is reduced. Now, the power is the product of the head extraction and the mass flow, so that extraction of a large amount of head will result in the mass flow being necessarily reduced. In practice, this means that the far downstream slip stream will be found to have a speed close to zero with consequent reductions in the mass flux. In classical wind turbine theory this is referred to as operation in the windmill brake state. However, it appears that for some augmentor systems viscous effects make it possible to extract more power than that associated with the inviscid limit. This situation can be illustrated by reference to the ducted augmentor.

It appears here that large head extraction can be accomplished, resulting in very slow inviscid slip stream speeds which would approach the recirculation situation if there were no viscous effect. However, if there is turbulent entrainment between the slip stream and the outer flow, then the flow velocity in the slip stream behind the turbine can be increased so that the mass flow in the wake is increased and the wake is scavenged and swept downstream. This presents an interesting situation where the wake flow is actually reenergized by the outer flow and, thus, some of the actuator power is an indirect result of power extraction from flow which did not actually go through the actuator. This phenomenon seems most pronounced for augmented systems and we can explain this as follows: At the actuator, a certain proportion of the local kinetic head can be extracted kinematically, but far downstream the final wake velocity will be determined by the speed which corresponds to the reduction of total head of the flow; that is, it is connected to the free stream global kinetic head. Thus, if one could extract, say, 30% of the local kinetic head in a flow of twice free stream speed (due to an augmentor), then 120% of the free stream kinetic head would have actually been removed. Theoretically, in an inviscid flow,

this could not occur in the far downstream wake, where full stagnation would correspond to removal of 100% of the free stream kinetic head by energy entrainment from the outer flow. However, it appears that, after power extraction, the wake total head can be increased. Thus, it seems plausible that, with augmentors, the possibility of extracting a larger amount of the local dynamic head occurs, provided there is some turbulent mixing process in the wake of sufficient entrainment capacity to restore the wake speed to some positive value in the direction of the flow.

It is believed that the fundamental principles of the augmentor, described above, will make it possible to analyze the optimum requirements of an augmentor from the basic fluid-mechanical ideas. Thus, application of the above concepts makes it possible to logically configure an optimal augmentor system, rather than by analysis of various postulated good configurations. This morphological approach may make it possible to determine whether any augmentor configurations of high potential have been overlooked.

5.2 COMPARISON OF SYSTEMS ANALYZED

Using the ideas outlined above, and employing current structural cost estimates, we can calculate the plant cost and power cost of the various systems. These results are shown in Table 3-8. It is noted that the standard propeller-type system (Mod-X) appears distinctly superior to both forms of static inducer, and marginally better than the dynamic inducer. It is seen that the disadvantage in the case of the static inducers is the high cost of the inducer itself, which constitutes about 85% of the cost of the system and is not cost-effective in the additional power it produces.

We conclude that the cost of the static inducer surfaces must be reduced by a factor of between 3 and 10 for the system to be cost-effective compared to the Mod-X. It appears unlikely that this is possible. It is noted here that rather optimistic estimates of the aerodynamic performance have been made, so that further effort to make these systems cost-effective should relate to structural cost-reduction. It appears that these cost reductions are larger than seems achievable. However, the static inducer systems may show more attractive cost figures when operating in high wind regimes, since the power output will increase but not the inducer cost, because it is already designed for high winds.

It is noted that for all the inducer systems, improved rotor efficiencies will be very advantageous because of the increased flow speeds at the rotor. The dynamic inducer will particularly benefit from increased rotor efficiency since this will reduce the viscous losses due to the tip-vanes or inducer blades compared to total rotor output. In addition, this increased efficiency will decrease the system drag, thus reduce the tower load and, consequently, its cost. It is believed that improved rotor viscous efficiency will make the dynamic inducer cost-effective. As an illustration, a previous study by AeroVironment for the dynamic inducer (Lissaman and Walker, 1978) assumed 100% rotor efficiency for both the augmented and baseline systems, with the result that the dynamic inducer was 6% more cost-effective than the comparable free turbine.

It is noted here that augmented systems should always be compared on an equal-power-output basis, as has been done here, and not on an equal-rotor-diameter basis. The equal rotor diameter comparison leads to the deceptive concept of "X times the power from the same rotor," which does not take into account the increased costs of tower, power train, and generator. This will bias the results, since cost comparison for the same diameter rotor will involve different rated powers, capacity factors, and other variables. An

unbiased result would be to compare machines of the same rated power; this is the method used in this report. This bias will tend to make the system with the highest induction look the best, whereas a proper, equal power comparison will show the true cost trends.

It is further noted that all the extrapolated "maximum power coefficient" systems are more effective than the high confidence systems. But these maximum power coefficient systems involve operation at very high rotor kinetic head extraction levels, involving situations close to, or in the windmill brake state, which are not possible in inviscid flow and which involve turbulent entrainment scavenging. Various test data suggest that this scavenging does, in fact, occur even for free wind turbines. However, the fluid mechanics of this state are poorly understood and more research is required here.

Finally, it is noted that while none of the systems have been exhaustively analyzed structurally for cost estimation, it is likely that the structured estimates for the dynamic inducer are most reliable, since the tip-vanes are more similar to standard rotor blades than are static inducer surfaces. It is noted further that if the "blade-locked gale" case is taken as a design criterion, then the dynamic inducer is likely to have an even greater advantage than the other systems because its surface area is much smaller and presents less drag surface normal to the wind. For example, in the theoretical gale, the surface area to be considered for survival for the axisymmetric static inducer is 18 times that of the dynamic inducer, while the planar static inducer has 60 times the area.

From an aerodynamic point of view, quite extensive work has been done on both types of static inducer, and the high confidence power augmentation has been proven. This is not the case with the dynamic inducer, where no actual power augmentation has been demonstrated. It must be clearly noted here that experimental work on complete dynamic inducer systems is very limited and no comprehensive, systematic tests on the complete unit have ever been performed. However, the principles of flux amplification have been experimentally proven, and it has also been experimentally shown that the dynamic induction system can be driven at relatively low power levels (van Holten, 1978). It is these experimental results, as well as theoretical considerations, that were used to predict the performance of the dynamic inducer system analyzed in this report. It is stressed that, of the three systems considered, the dynamic inducer has had, by far, the least dynamic research and development.

On these grounds, taking into account the fact that the analyses here show that the dynamic inducer is comparable to the baseline system, it is believed that further work is justified to refine the aerodynamic and structural analysis.

5.3 RECOMMENDATIONS FOR RESEARCH AND DEVELOPMENT ON AUGMENTORS

The preceding sections have outlined the current conclusions regarding augmentor devices, and identified the areas of uncertainty, of high promise and of serious disadvantage. It is believed that in most of the technology, passable estimates (possibly within a factor of 50%) can be made. Therefore, it is appropriate now to concentrate on certain types and to focus the scope of innovative research to major programs on the most promising systems, while still maintaining a low level funding in high risk fundamental exploratory research.

It is recommended that research in the following areas should be conducted:

- High Power Output Rotors Operating in the Windmill Brake State. It has been shown that augmentor rotors can benefit from operating in the brake state. This brake state apparently involves turbulent entrainment from the outer

flow, thus making additional energy available to the actuator. Analytical and experimental work is appropriate here with special attention to turbulent effects. It is noted that this research would also have considerable bearing on the understanding of the development of wind turbine wakes, which is important in constructing models for the performance of arrays of wind turbines.

A research program to investigate the brake state is recommended. It is important that the analytical and experimental work be conducted concurrently and in conjunction; thus, this should be a single program.

- Increased Rotor Efficiency for Augmented Systems. It has been noted that augmented systems are particularly benefitted by increased rotor efficiency, which will presumably come from using airfoil sections of lower profile drag and higher lift. This work can be performed on two-dimensional airfoils and should be both analytical and experimental. This research can be coupled with the development of airfoil sections for vertical axis machines.

It should be noted that these improvements to the rotor involve changes in rotor airfoil sections and possibly planform, and thus have only a minor influence on rotor costs. It is possible that these changes may result in a decrease in blade area and, hence, lower blade costs. However, if these performance increases do result in increased rotor costs, it is expected that these higher costs will be more than offset by the performance increase. This can be seen as follows: For augmented systems, the rotor cost has been reduced to a very small value. A small increase in rotor cost will result in an almost insignificant increase in total system costs. The increased performance will result in lower inducer costs. The inducer has been found by this study to be the major cost item in an augmented system. Thus, almost any increase in rotor performance will result in a lower system cost.

A research program to investigate advanced airfoils and optimized planforms is recommended. Because of the discrete nature of the work, it is believed that it would be desirable to have a number of contractors, each operating independently, working to develop the best airfoil classes to meet well-defined lift and Reynolds number specifications.

- Cost Estimates for Static Inducer Surfaces. It has been shown that the Static Inducer surface represents a major cost element in those systems, but the precision of cost estimation is not known. However, a large amount of experience on wind-loaded surfaces does exist in the construction and aerospace industry. It is believed that a more comprehensive cost estimate of these inducer structures should be made, using both fundamental design principles and statistical data from comparable wings and ducts to size the components.

A research program to investigate these cost parameters is recommended. Here, it is suggested that at least two independent programs be initiated as a mutual check. It is noted that a precision of higher than 20% is not required, since the static inducers can only be effective if costs are reduced by much larger factors.

- Aerodynamic Development of Dynamic Inducers. It has been shown that the dynamic inducer represents the most potentially attractive inducer system;

yet experimental test data is lacking and the aerodynamic performance has had to be estimated from a combination of various component performances. It is recommended that analytical, experimental and, if justifiable from the results of the above studies, field test research should be performed to develop inducer tip-vane geometry, to integrate the tip-vanes with the power blades, and to design and operate the complete system.

This research program should include analytical performance modeling, wind tunnel component testing, and field testing of complete units. Because of the integrated nature of this system, it is appropriate for the major portion to be conducted by one contractor, but certain subelements, relating to airfoil design for low drag in rotating flows, can be performed by subcontract or on separate contracts.

- Aeroelastic Analysis of Dynamic Inducers. If the aerodynamic performance of the dynamic inducer proves attractive, then it will be necessary to determine if there will be any aeroelastic problems. At the present level, the aeroelastic study can be made prior to a complete detailed definition of the dynamic inducer system, since the basic geometry can be specified now. An analytical study, using available aeroelastic computer models (which will be adequate after being modified for this geometry), should be performed.

This research program should be done analytically as described above, and should be performed in detail for a selected optimal configuration and, in more general terms, for a parametric range of blade geometry, tip speeds, and rotor diameter.

- Improved Cost Analysis of Dynamic Inducer Rotor. The current method of cost estimating power blades and tip-vanes for dynamic inducer systems is based on ordinary horizontal axis rotor systems. However, the tip-vanes experience a complex load system due to inertial and aerodynamic effect and, in addition, introduce special dragwise and radially-inwards loads on the power blades, which are not normally present for ordinary rotors. Thus, the blade loading will be different, and it is to be expected that this will have an effect in blade cost.

A research program is recommended which would involve a relatively detailed load estimation for the blade and inducer components for various design cases, and an estimation of the blade cost using a combination of rational structural analysis with statistical data for ordinary wind turbine blades.

- General Study of Potential of Inducer Systems. The work already performed has shown that different types of inducer do, in fact, increase the power output of a rotor, although at an increased cost which is associated with the inducer geometry. However, the systems studied to date have been specific configurations, not necessarily optimized for maximum efficiency. It is believed that sufficient basic understanding of the aerodynamics and structural cost is now available, so that a wide ranging morphological study of inducers can be made, with a view to identifying configurations having optimal characteristics, just as this can be done for lifting surfaces.

A research program is recommended which should involve analytical work only, and should be aimed at investigating the basic features of optimal

inducers, with first order cost estimates of such systems. In essence, this would be a high-risk exploratory program intended to identify any promising configurations which may have escaped attention to date.

SECTION 6.0

CONCLUSIONS AND RECOMMENDATIONS

The conclusions and recommendations are summarized below in abbreviated form. The reasons and detailed explanation of these statements have already been given.

- Of the three systems analyzed, the dynamic inducer was the only one with cost-effectiveness comparable to the baseline Mod-X, an advanced horizontal axis conventional wind turbine. A dynamic inducer using high confidence performance figures has a power cost ratio of about 1.2 of the baseline. The power cost ratio of the static inducer systems was about two to five times that of the baseline unit.
- For the static inducers, the aerodynamic performance is quite well understood, and test data is available. For the dynamic inducers, although theoretical performance estimates are promising, no test data is available for the complete system. However, test data for subsystems of the dynamic inducer is available, and has supported analytical estimates. It is noted that much less research has been performed on the dynamic inducer system than on the others.
- Structural analysis and cost estimation of the various inducer systems is still quite imprecise and statistical cost data is lacking. However, it is believed that cost reduction by a factor of 2 or 3, which is the amount required to make some of the inducer systems cost-effective, will be very difficult to achieve.
- An understanding of the general mechanisms of inducers has been obtained, and the importance of turbulent effects for highly loaded rotors has been identified.
- It is recommended that research on innovative inducer systems should concentrate on the most cost-effective device, the dynamic inducer.
- A short-term research program has been outlined, designed to investigate only those areas which show the most promise. These areas involve:
 - Dynamic inducer aerodynamics, aeroelasticity, and structural cost.
 - Study of windmill brake states for heavily loaded rotors, and improvement of rotor efficiency.
 - Structural cost estimates to study the very high apparent costs of static inducer surfaces.
 - Limited high risk work on the identification of optimal inducer systems.

SECTION 7.0

REFERENCES

- Foreman, K. M., and B. L. Gilbert. Diffuser Designs for Improved Wind Energy Conversion. Reprint from Fluids Engineering in Advanced Energy Systems, edited by C. H. Marston, ASME; 1973.
- Foreman, K. M. DAWT Program Review - 1978. Private communication of proprietary material; 1979.
- Frost, W., B. H. Long, and R. E. Turner. Engineering Handbook on Atmospheric Environmental Guidelines for Use in Wind Turbine Generator Development. NASA Technical Paper 1359; December 1978.
- General Electric Company. Design Study of Wind Turbines 50 kW to 300 kW for Electric Utility Applications - Volume II - Analysis and Design. ERDA/NASA Report No. 9403-76/2; 1976.
- Justus, C. G., W. R. Hargraves, and A. Mikhail. Reference Wind Speed Distributions and Height Profiles for Wind Turbine Design and Performance Evaluation Applications. ORO/5108-76/4 UC 60; August 1976.
- Lissaman, P. B. S. General Performance Theory for Cross-Wind Axis Turbines. Proceedings of the International Symposium on Wind Energy Systems, British Hydro Mechanics Research Association, England; September 1976.
- Lissaman, P. B. S. Increased Windmill Performance with Tipvanes. (AV TP 636, AeroVironment Inc., Pasadena, CA); April 1976.
- Lissaman, P. B. S., and S. N. Walker. Dynamic Inducer Research Program. AeroVironment Inc., DOE Contract RLO/1021-77/1; June 1978.
- Lockheed Aircraft Company. Wind Energy Mission Analysis. ERDA Report No. SAN/1075-1/1; 1976.
- Loth, J. L. Betz Type Limits for Vortex Wind Machines. From Third Wind Energy Workshop; 1977.
- NASA Technical Report. 200-kW Wind Turbine Generator Conceptual Design Study. DOE/NASA/1028-79/1; NASA TM-79032; January 1979.
- Sforza, P. M. Vortex Augmentor Concepts for Wind Energy Conversion. From Second Wind Energy Workshop; 1976.
- Sforza, P. M., and W. Stasi. Wind Power Distribution, Control, and Conversion in Vortex Augmentors. Reprinted from Fluids Engineering in Advanced Energy Systems, edited by C. H. Marston, ASME; 1978.
- vanBussel, G. J. W., T. van Holten, and G. A. M. van Kuik. Flow Visualization Study of the Functioning Tipvanes. Delft Institute of Technology, Memorandum M-295, The Netherlands; February 1978.

- van Holten. Performance of a Windmill with Increased Power Output Due to Tipvane Induced Diffusion of the Airstream. Delft Institute of Technology, Memorandum M-224, The Netherlands; November 1974.
- van Holten, T. Works Done by the "Tipvane-Group" of the Delft University of Technology for the National Research Program Windenergy. Memorandum M-305, The Netherlands; May 1978.
- Wilson, R. E., P. B. S. Lissaman, and S. N. Walker. Aerodynamic Performance of Wind Turbines. Oregon State University report supported by the National Science Foundation, Research Applied to National Needs (RANN) Under Grant No. AER-74-04014-A03; June 1976.